

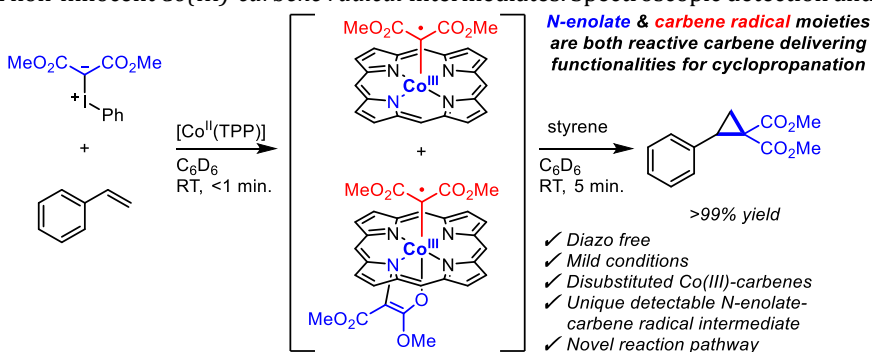
# [Co(TPP)]-Catalyzed Carbene Transfer from Acceptor-Acceptor Iodonium Ylides via *N*-enolate Carbene Radicals

Roel F.J. Epping, Mees M. Hoeksma, Eduard O. Bobylev, Simon Mathew and Bas de Bruin\*

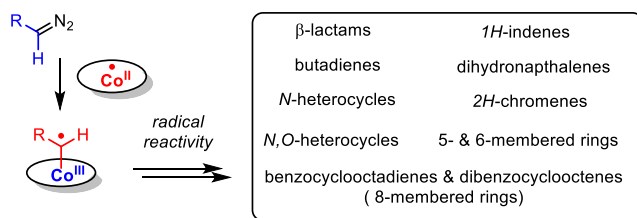
Homogeneous, Supramolecular and Bio-Inspired Catalysis Group, Van 't Hoff Institute for Molecular Sciences (HIMS), University of Amsterdam, Science Park 904, 1098 XH Amsterdam, The Netherlands

KEYWORDS: carbene radical, iodonium ylides, cobalt catalysis, cobalt porphyrin, cyclopropanation, mechanistic studies

**ABSTRACT:** Square-planar cobalt(II)-systems have emerged as powerful carbene transfer catalysts for the synthesis of a variety of (hetero)cyclic compounds via redox non-innocent *Co(III)*-carbene radical intermediates. Spectroscopic detection and characterization of these reactive carbene radical intermediates has thus far been limited to a few scattered experiments, in part due to the fact that most studies have focused on *mono*-substituted carbene precursors. In this work, we demonstrate the unique formation of *disubstituted cobalt(III)*-carbene radicals in reactions between a cobalt(II)-porphyrin complex with acceptor-acceptor  $\lambda^3$ -iodaneylidenes (iodonium ylides) as the carbene precursors. We report detailed spectroscopic characterization of the resulting reactive carbene radical species, and their application in styrene cyclopropanation. In particular, we demonstrate that iodonium ylides generate novel *bis*-carbenoid species leading to *reversible* substrate-promoted ligand modification of the commercially available [Co(TPP)]-catalyst. Two interconnected catalytic cycles are involved in the overall catalytic reaction with a *mono*-terminal carbene radical and an unprecedented *N*-enolate-carbene radical intermediate as the respective key species for the *mono*- and *bis*-carbene cycles. Notably, *N*-enolate formation is *not* a catalyst deactivation pathway, and both the *N*-enolate and the carbene radical moieties can be transferred as carbene units to styrene. The studies provide a detailed picture of the new [Co(TPP)]-catalyzed carbene transfer reactions from iodonium ylides. The findings are supported by detailed and unequivocal characterization of the reactive *N*-enolate & carbene radical intermediates and their deactivation products (EPR, UV-Vis, HR-MS, NMR, in-situ ATR-FT-IR, SC-XRD), Hammett analysis, mechanistic control experiments, DFT reaction pathway profiling and NEVPT2-CASSCF electronic structure calculations.

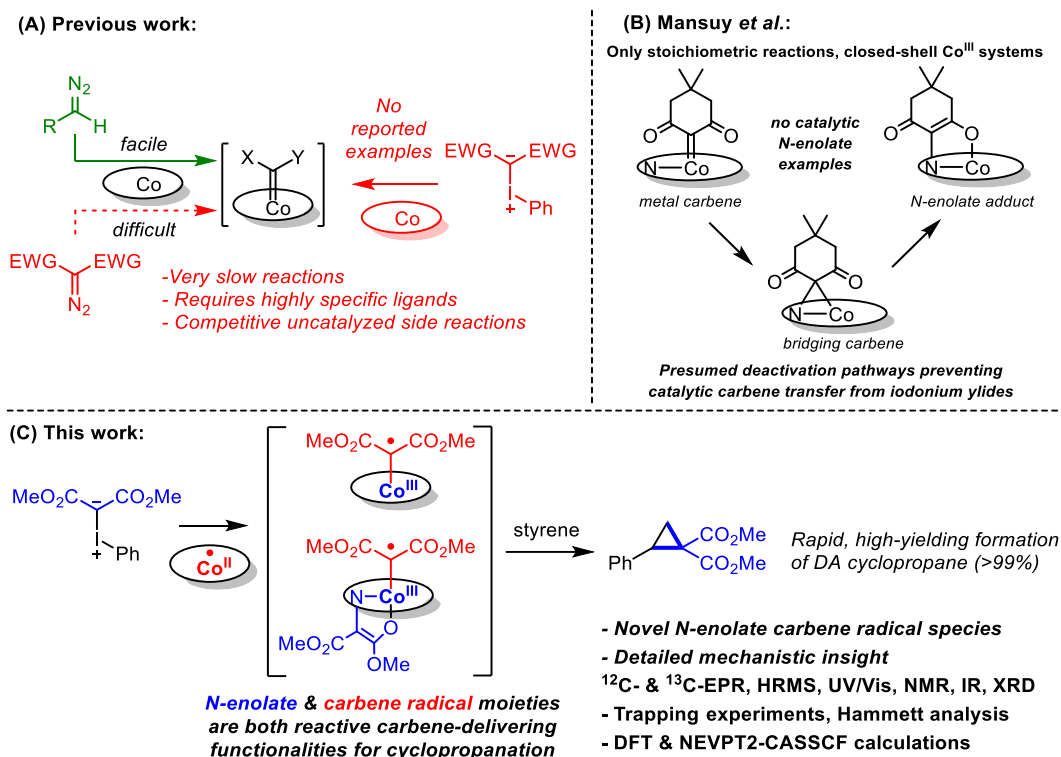


**Introduction:** Carbon-carbon bond formation is at the heart of synthetic organic chemistry. While traditional methods have provided a plethora of reliable approaches, direct functionalization of unactivated C-H bonds,<sup>1</sup> or access to strained and medium-sized carbocycles and heterocycles remains a difficult task.<sup>2</sup> In this perspective, transition metal Fischer-type carbenes have emerged over several decades as highly versatile intermediates to directly access a variety of motifs. Their synthetic utility ranges from cyclopropanes to numerous C-H and X-H insertion reactions (X = O, N, S, Si), as well as several ring-closing and expansion reactions.<sup>3</sup> Previous work has focused mostly on platinum-group metals such as Rh<sup>4</sup> and Ru<sup>5</sup> and such systems are still among the most successful ones. Over the past



**Scheme 1.** Single-electron transfer from cobalt to the carbene moiety, enabling radical reactivity that has led to the successful synthesis of a variety of carbo- and heterocycles.

decades, attention has shifted largely towards 1<sup>st</sup>-row transition metals with a higher abundance and lower toxicity compared to their 2<sup>nd</sup>- and 3<sup>rd</sup>-row counterparts.



**Scheme 2.** (A) Transition metals employed previously in catalysis using *mono/bis*-substituted diazo substrates and iodonium ylides. (B) Coordination chemistry of acceptor-acceptor metal carbenes leading to *N*-enolate species (Mansuy *et al.*). (C) Application of iodonium ylides in *cobalt*-catalyzed cyclopropanation with detailed mechanistic insight revealing novel *N*-enolate type carbene radical species that yield donor-acceptor cyclopropanes in quantitative yield. Notably, both the carbene radical and the *N*-enolate moieties are reactive carbene-delivering functionalities capable of carbene transfer to styrene.

Most of these are  $\text{Cu}^{\text{I}}$ - and  $\text{Fe}^{\text{II}}$ -based systems, which typically react via classical Fischer-type carbenes, similar to the reactivity of noble-metal catalysts. However, specific base metals give access to novel and different reactivity via alternative reaction pathways. Particularly, cobalt systems have shown to be of special interest, as they tend to react via single-electron radical-type pathways that provide new and useful catalytic protocols.<sup>8</sup> Specifically cobalt-porphyrin complexes such as  $[\text{Co}(\text{TPP})]$  (cobalt(II)-tetraphenylporphyrin) have shown to be useful for a variety of cyclization reactions that are mostly inaccessible with traditional Fischer-type carbene chemistry. This includes the synthesis of electron deficient olefin-based cyclopropanes,<sup>9</sup>  $\beta$ -lactams,<sup>10</sup> indenes,<sup>11</sup> *2H*-chromenes,<sup>12</sup> piperidines,<sup>13</sup> 8-membered rings<sup>14</sup> and various other motifs (Scheme 1).<sup>15,16,17,18,19</sup> At the core of this chemistry is a metal-to-substrate single-electron transfer process, from the cobalt center to the carbene moiety, which imbues the carbene with radical properties. The resulting carbene radical intermediate proceeds to react via single-electron, stepwise radical type pathways with various substrates as opposed to conventional two-electron reactivity (Scheme 1).<sup>20</sup>

Due to their reactive nature, spectroscopic detection and characterization of the carbene radical intermediates has been limited to a few scattered experiments, mostly involving the detection of minor amounts at low temperatures to-

gether with other species (including 'bridging carbenes')<sup>20a,21</sup> or indirect detection with spin trapping agents.<sup>9m,14a</sup> This can be partially explained by the fact that in most of these studies *mono*-substituted carbene precursors were used, which provide limited steric protection and/or electronic stabilization. Disubstituted carbenes, and in particular acceptor-acceptor carbenes are anticipated to have a (radical) stabilizing effect, thus facilitating detection and characterization of the key reactive intermediates. Furthermore, development of efficient protocols for carbene transfer from disubstituted carbene precursors would also expand the scope of cobalt(II)-catalyzed group transfer reactions substantially.

However, in almost all reported catalytic reactions the reactions are restricted to the use of *mono*-substituted diazo compounds as carbene precursors. Activation of disubstituted acceptor-acceptor diazo compounds has proven to be far more difficult (Scheme 2A). The Zhang group developed enantioselective porphyrins equipped with hydrogen-bond donor motifs that facilitate carbene radical formation,<sup>22</sup> and some of these can activate specific disubstituted diazo compounds. However, this remains in general a challenging task, as the complexity of these catalysts demand lengthy syntheses and also the inherent toxicity and potentially explosive nature of diazo compounds calls for development of alternative approaches. As such, hypervalent iodine(III) an-

alogues (i.e. iodonium ylides) are useful alternative precursors for carbene formation.<sup>23,24</sup> The outstanding nucleofugality of iodobenzene ( $10^6$  times greater leaving group capability than triflate<sup>25</sup>) facilitates metal carbene formation, providing a distinct advantage for carbene transfer reactions involving disubstituted acceptor-acceptor carbenes.<sup>26,27,28,29,30</sup> However, to the best of our knowledge, there are no reported examples of homogeneous cobalt systems capable of catalytic carbene transfer from iodonium ylides (Scheme 2A).<sup>31</sup> For Fe<sup>II</sup>- and closed-shell Co<sup>III</sup>-porphyrin-based systems, a likely reason for this behavior is the observed formation of catalytically inactive *N*-enolate species, as described by Mansuy and coworkers (Scheme 2B).<sup>32</sup> They investigated the organometallic chemistry of closed-shell Co<sup>III</sup> and (integer-spin) Fe<sup>II</sup>-porphyrin systems in the presence of acceptor-acceptor iodonium ylides, and found that the cyclic diester carbenes rapidly rearrange to *mono*- or *bis-N*-enolate modified porphyrins with the pendant carbonyl group serving as the 5<sup>th</sup> or 6<sup>th</sup> ligand (Scheme 2B). None of these reported *N*-enolate structures is catalytically active, and hence it is tempting to consider the reaction shown in Scheme 2B as a general catalyst deactivation pathway when using acceptor-acceptor carbenes. Herein we demonstrate that this assumption is incorrect for open-shell cobalt systems.

Building on the prior art described above, we decided to investigate the catalytic carbene transfer from acceptor-acceptor iodonium ylides mediated by homogeneous cobalt(II)-based systems, which uncovered an efficient protocol for styrene cyclopropanation via unique radical-type reaction intermediates (Scheme 2C). In this combined experimental, spectroscopic and computational study we aim to answer the following research questions:

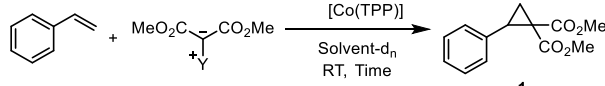
- 1) Can iodonium ylides be used in [Co(TPP)]-catalyzed cyclopropanation of styrene and how do they compare to analogous diazo compounds?
- 2) What is the mechanism behind these reactions and how does this compare to contemporary Co<sup>III</sup>-carbene radical mechanisms?
- 3) Do *N*-enolate species also play a role in the reactivity of open-shell Co<sup>II</sup>-species and can they be detected?
- 4) What are the active species, ruling reaction mechanisms and dominant deactivation pathways of these catalytic reactions?

**Results and Discussion:** We first set out to test the catalytic activity of [Co(TPP)] in the cyclopropanation of styrene using either dimethyldiazomalonate (DMM•N<sub>2</sub>) or dimethylmalonate iodonium ylide (DMM•IY) as a model reaction (Table 1). The diazo substrate yielded little to no cyclopropane product (<10%, based on <sup>1</sup>H-NMR) even when heated to 60 °C for 60 h (Entry 1 & 2). This reactivity is consistent with previously reported attempts to activate acceptor-acceptor diazo compounds.<sup>33</sup> In marked contrast, the analogous reaction using the corresponding iodonium ylide yielded 99% cyclopropane in <1 h at 20 °C (Entry 3). Further screening of solvents (Entry 3–10) revealed that apolar solvents work best, of which C<sub>6</sub>D<sub>6</sub>, CD<sub>2</sub>Cl<sub>2</sub> and toluene-*d*<sub>8</sub> gave the highest yields. Temporal reaction monitoring (Figure S6, Supp. Inf.) shows slightly higher yields in C<sub>6</sub>D<sub>6</sub> than

in non-deuterated benzene. Optimization of the catalyst loading, DMM•IY equivalents and time (Entry 11–16) revealed that quantitative yields can be obtained with a 2.5 mol% catalyst loading in just 5 minutes.

Several control experiments confirm a crucial role of the [Co(TPP)] catalyst, and reactions in the presence of air or TEMPO as a trapping agent gave rise to reduced or no yield, respectively, confirming that radical-type reactions are operative. Unsurprisingly, when using only the malonate or the PIDA (phenyliodosodiacetate) reagent no cyclopropane product was detected. However, when combining both compounds together with 6 eq. of KOH as a base, a small amount of product was observed, ascribed to in situ formation of the ylide (Table S7, Supp. Inf.).

**Table 1.** Screening of carbene precursors (Y = N<sub>2</sub> or IPh) in the cyclopropanation of styrene with [Co(TPP)] and optimization of reaction conditions using DMM•IY.



Entry	cat. loading (mol%)	solvent	Y	Time (min.)	Yield (%) <sup>a</sup>
1	5	C <sub>6</sub> D <sub>6</sub>	N <sub>2</sub>	60	0 ± 0%
2	5	C <sub>6</sub> D <sub>6</sub>	N <sub>2</sub>	3600	10 ± 3%
3	5	C <sub>6</sub> D <sub>6</sub>	IPh	60	99 ± 4%
4	5	Tol- <i>d</i> <sub>8</sub>	IPh	60	98 ± 5%
5	5	CD <sub>2</sub> Cl <sub>2</sub>	IPh	60	98 ± 1%
6	5	CDCl <sub>3</sub>	IPh	60	66 ± 4%
7	5	THF- <i>d</i> <sub>8</sub>	IPh	60	58 ± 0%
8	5	DMSO- <i>d</i> <sub>6</sub>	IPh	60	84 ± 1%
9	5	CD <sub>3</sub> OD	IPh	60	4% <sup>b</sup>
10	5	CD <sub>3</sub> CN	IPh	60	31% <sup>b</sup>
11	5	C <sub>6</sub> D <sub>6</sub>	IPh	60	81 ± 4% <sup>c</sup>
12	5	C <sub>6</sub> D <sub>6</sub>	IPh	5	99 ± 3%
13	2.5	C <sub>6</sub> D <sub>6</sub>	IPh	5	99 ± 1%
14	2.0	C <sub>6</sub> D <sub>6</sub>	IPh	5	79 ± 1%
15	1.0	C <sub>6</sub> D <sub>6</sub>	IPh	5	48 ± 1%
16	0.1	C <sub>6</sub> D <sub>6</sub>	IPh	5	4 ± 1%

<sup>a</sup> Yields based on <sup>1</sup>H-NMR integration using 1,3,5-trimethoxybenzene as an internal standard. Performed in duplicate; <sup>b</sup> Single run experiment; catalyst poorly soluble; <sup>c</sup> 1:1 styrene: DMM•IY.

**Mechanistic investigations.** Based on previous work regarding hypervalent iodine reagents in cobalt-catalyzed nitrene transfer,<sup>34</sup> we suspected that *bis*-carbenoid intermediates might play a role in catalysis.<sup>35</sup> This was initially investigated using positive-mode cold electrospray ionization high resolution mass spectrometry (ESI<sup>+</sup>-HR-MS). Identical to catalytic conditions, 24 eq. of solid DMM•IY were mixed with a solution of [Co(TPP)] in benzene (4.5 mM) and measured with ESI<sup>+</sup>-HR-MS (Figure 1A).

Two major peaks at  $m/z = 801$  Da and  $m/z = 931$  Da match those of *mono*- and *bis*-carbenoid complexes, respectively. The isotopic patterns are in line with *mono*-cationic ions and subsequent reduction of the ionization voltage resulted in a complete collapse of both signals, suggesting the ionization of neutral species. Peaks at  $m/z = 671$  and  $1620$  Da, respectively, match that of the free [Co(TPP)] catalyst and a water adduct of a dimeric form of the *mono*-carbenoid species (Figure S27, Supp. Inf.). MS-MS analysis (Figure S37, Supp. Inf.) shows  $m/z = 671$  Da and  $m/z = 801$  Da to be fragments of  $m/z = 931$  Da. However, the presence of some *mono*-carbenoid species cannot be excluded solely on the basis of these MS experiments.

To shed more light on the stoichiometry of the reaction, UV/Vis spectroscopy was used to probe changes in the porphyrin's Soret and Q-bands. Titrating the [Co(TPP)] catalyst with 0 to 2.5 eq. of DMM•IY in CH<sub>2</sub>Cl<sub>2</sub> revealed a transition of the Soret peak at 410 nm to 430 nm (significantly lower intensity), with isosbestic points at 383, 424, 518 and 542 nm (Figure 1B). Full conversion is observed with 2 eq. of the iodonium ylide, above which the spectrum does not change anymore. This reveals rapid formation of a single, new species without a detectable second, long-lived intermediate. The Q-band at 528 nm fully collapses into the baseline. Coupled with the red-shift of the Soret peak, this points to a substantial perturbation of the (electronic) structure of the porphyrin macrocycle induced by oxidation of Co<sup>II</sup> to Co<sup>III</sup> with a concomitant chemical reaction between a carbene moiety and the porphyrin ring.<sup>32,34a</sup> We ascribe this to selective formation of *N*-enolate-carbene radical species I<sup>E-T</sup> (Scheme 3). Additional support by TD-DFT calculations corroborates these findings (p. S75, Supp. Inf.).

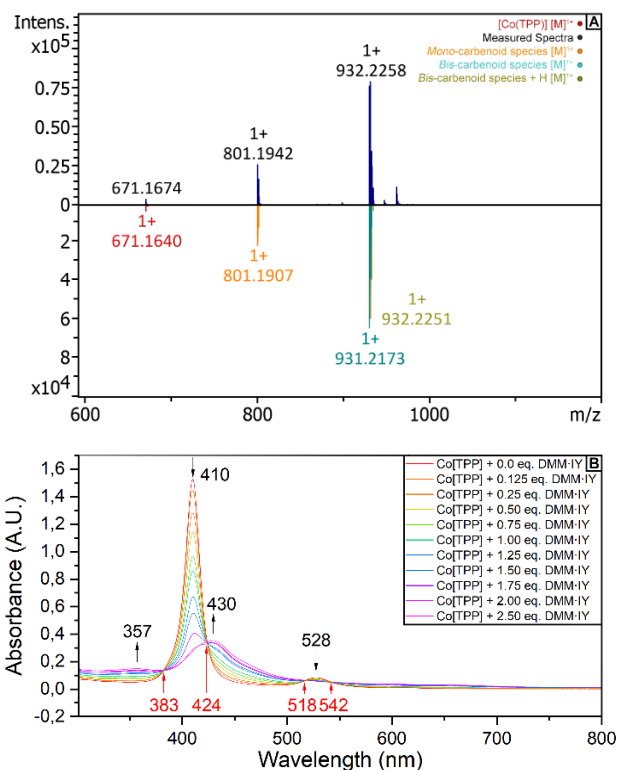
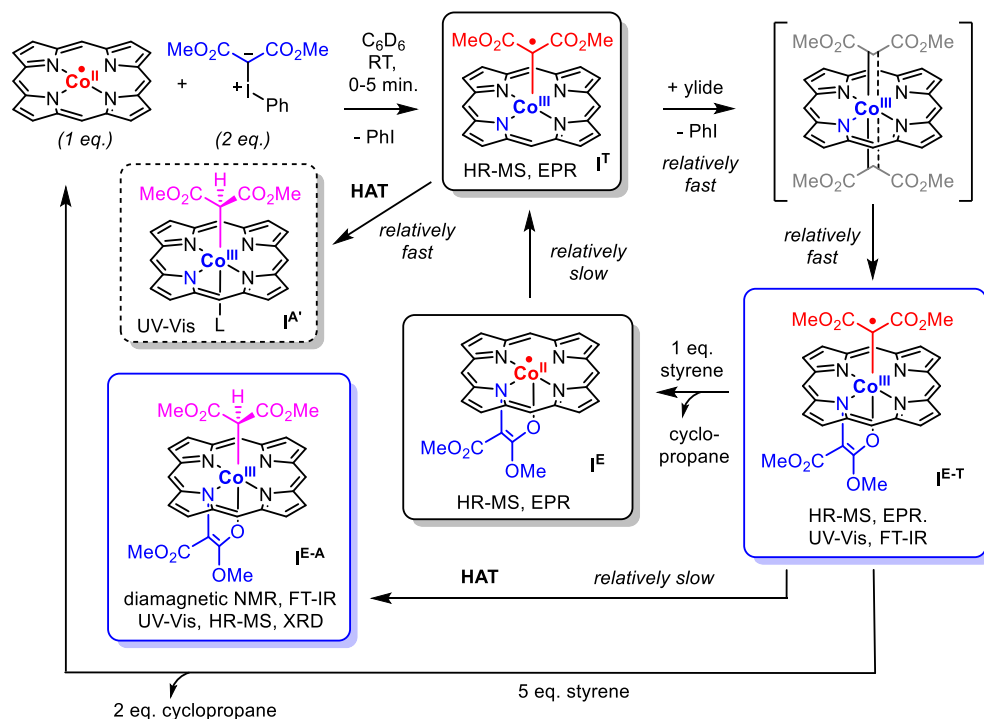


**Figure 1.** (A) CSI<sup>+</sup>-HR-MS spectrum of a reaction between [Co(TPP)] and DMM•IY, illustrating the presence of *mono*- ( $m/z = 801$  Da) and *bis*-carbenoid complexes ( $m/z = 931$ ;  $932[+H^+]$ ) and residual (or fragmentation to) [Co(TPP)] ( $m/z = 671$ ). (B) UV/Vis spectra of a series of reactions between [Co(TPP)] and varying equivalents of DMM•IY in CH<sub>2</sub>Cl<sub>2</sub> at  $t = 0$  min.



**Scheme 3.** Formation of *N*-enolate-carbene radical I<sup>E-T</sup> obtained by reaction between [Co(TPP)] and DMM•IY, based on the spectroscopic evidence (EPR, UV/Vis, CSI<sup>+</sup>-HR-MS and in-situ ATR-FT-IR). The *mono*-terminal carbene radical intermediate I<sup>T</sup> is not detectable during UV-Vis titrations leading to formation of I<sup>E-T</sup>, but can be detected in single turnover experiments between I<sup>E-T</sup> and 1 eq. styrene. Complex I<sup>E-T</sup> deactivates to diamagnetic *N*-enolate-alkyl species I<sup>E-A</sup> via HAT (e.g. from toluene). Phenyl rings of the TPP ligand omitted for clarity.

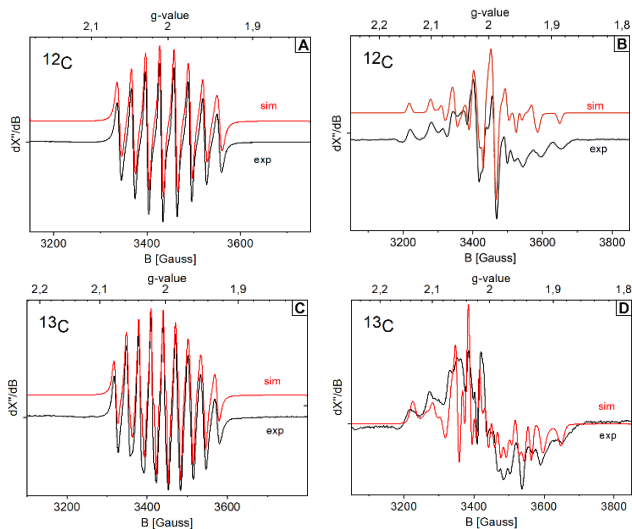


**Figure 2.** (A) Experimental (black) and simulated (red) X-band EPR spectrum of species  $\text{I}^{\text{E-T}}$  obtained in a reaction between  $\text{DMM}\cdot\text{IY}$  and  $[\text{Co}(\text{TPP})]$  in benzene at RT (Microwave freq. 9.6434 GHz, mod. amp. 1 G, power 20 mW). (B) Spectrum of  $\text{I}^{\text{E-T}}$  measured in toluene glass at 40 K (Microwave freq. 9.6435 GHz, mod. amp. 4 G, and power 0.633 mW). (C) Spectrum of  $^{13}\text{C}\text{-I}^{\text{E-T}}$  measured at RT of the reaction between  $^{13}\text{C}\text{-DMM}\cdot\text{IY}$  and  $[\text{Co}(\text{TPP})]$  in benzene at RT (Microwave freq. 9.6449 GHz, mod. amp. 4 G, power 0.633 mW). (D) Spectrum of  $^{13}\text{C}\text{-I}^{\text{E-T}}$  measured in toluene glass at 40 K (Microwave freq. 9.6429 GHz, mod. amp. 4G, power 0.633 mW). Simulated parameters are mentioned in the text and are listed in Table S5.

To further investigate the potential role of radical species  $\text{I}^{\text{E-T}}$ , we turned to X-band EPR spectroscopy. At room temperature in benzene, an isotropic spectrum (Figure 2A) was acquired that is characteristic of a  $S = 1/2$  system with small  $^{59}\text{Co}$  hyperfine interactions (HFIs) ( $A^{\text{Co}_{\text{iso}}} = 85.6$  MHz) and an isotropic  $g$ -value ( $g_{\text{iso}} = 1.998$ ) indicative of a cobalt-bound but organic-centered radical undergoing restricted tumbling in solution (Figure 2A). Additional EPR measurements at 40 K in toluene glass (Figure 2B) showed a complex HFI pattern and a rhombic  $g$ -tensor. A satisfactory simulation was obtained revealing parameters matching that of a cobalt-bound, organic-centered radical ( $g_{11} = 1.997$ ;  $g_{22} = 2.006$ ;  $g_{33} = 2.008$ ). The spectrum is in line with an  $S = 1/2$  system with small  $^{59}\text{Co}$ -HFIs ( $A^{\text{Co}_{11}} = 21$ ,  $A^{\text{Co}_{22}} = -173$ ;  $A^{\text{Co}_{33}} = -103$  MHz).  $^{13}\text{C}$ -labeling of the ylidic carbon and reacting the  $^{13}\text{C}$ -labeled substrate  $^{13}\text{C}\text{-DMM}\cdot\text{IY}$  with  $[\text{Co}(\text{TPP})]$  in benzene gave a similar isotropic X-band EPR spectrum at room temperature as obtained for the  $^{12}\text{C}$ -analog, but now with 9 effective hyperfine lines instead of 8, which is caused by additional coupling with a *single*  $I = 1/2$   $^{13}\text{C}$ -nucleus (Figure 2C). Simulation revealed otherwise identical EPR parameters as obtained for  $\text{I}^{\text{E-T}}$  ( $^{13}\text{C}\text{-I}^{\text{E-T}}$ :  $g_{\text{iso}} = 1.998$ ,  $A^{59\text{Co}_{\text{iso}}} = 85.6$  MHz;  $A^{13\text{C}_{\text{iso}}} = 104.7$  MHz). The spectrum of  $^{13}\text{C}\text{-I}^{\text{E-T}}$  obtained in toluene glass at 40 K (Figure 2D) clearly indicates a splitting of the many HFI lines in the rhombic spectrum due to additional  $^{13}\text{C}$ -HFIs. As with the unlabeled spectra, simulation is indicative of a cobalt-bound but carbene-centered radical species ( $g_{11} = 1.998$ ;  $g_{22} = 2.004$ ;  $g_{33} = 2.006$ ).  $^{59}\text{Co}$ -HFIs match the previously obtained values ( $A^{\text{Co}_{11}} = 21$ ;  $A^{\text{Co}_{22}} =$

$-173$ ;  $A^{\text{Co}_{33}} = -103$  MHz), but with additional  $^{13}\text{C}$ -HFIs stemming from a single  $^{13}\text{C}$  nucleus ( $A^{13\text{C}_{11}} = 260$ ;  $A^{13\text{C}_{22}} = 30$ ;  $A^{13\text{C}_{33}} = 30$  MHz). These values are in good agreement with the DFT (B3LYP/ZORA-def2-TZVPP) calculated EPR parameters of the  $N$ -enolate-carbene complex  $\text{I}^{\text{E-T}}$  (Table S9, Supp. Inf.).

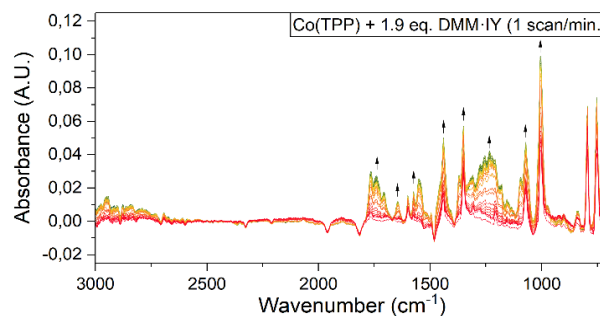


**Figure 3.** in-situ ATR-FT-IR spectrum of a supersaturated reaction between  $[\text{Co}(\text{TPP})]$  and  $\text{DMM}\cdot\text{IY}$  followed over time (1 scan/min.).

Complementary data were obtained with in-situ ATR-FT-IR studies. Addition of  $\text{C}_6\text{H}_6$  to a solid mixture of  $[\text{Co}(\text{TPP})]$  and  $\text{DMM}\cdot\text{IY}$  under continuous measurement revealed the appearance of a complex spectrum (Figure 3). Deconvolution of the spectra using DFT simulated IR spectra (BP86/def2-TZVP) and calibrated to known carbene IR frequencies<sup>36a</sup> (Table S11/S12, Supp. Inf.), revealed the splitting of the porphyrin's  $\beta$ -pyrrolic H-flipping, scissor, rocking and porphyrin stretching modes (742, 1071, 1207 and 1350  $\text{cm}^{-1}$  resp.) into two distinct peaks (734/754; 1062/1094; 1177/1209; 1354/1368  $\text{cm}^{-1}$  resp.), in agreement with desymmetrization of the porphyrin ring in  $\text{I}^{\text{E-T}}$ . On top of that, various peaks can be observed in the carbonyl stretching region typical for metal-alkyl and metal-carbene species with pendant ester groups.<sup>9b</sup> More specifically, two sets of peaks can be observed at 1573 and 1599  $\text{cm}^{-1}$  and 1738  $\text{cm}^{-1}$ . These are attributed to the metal carbene and metal alkyl species respectively. The additional peaks at 1705 and 1765  $\text{cm}^{-1}$  are tentatively assigned to a free- and coordinated alkyl dimer ( $\text{CH}(\text{CO}_2\text{Me})_2$ , respectively (Figure S22 and Table S12, Supp. Inf.). The peak at 1644  $\text{cm}^{-1}$  is attributed to the carbonyl stretching band of the free ester attached to the  $N$ -enolate carbene moiety as reported by Setune et al.<sup>36b</sup> and corroborated by our DFT results. The splitting of the porphyrin's  $\beta$ -pyrrolic and porphyrinic vibrational modes as well as the appearance of three distinct carbonyl peaks is in line with the conclusions derived from the above EPR studies. Ergo, on the basis of the combined spectroscopic evidence, we conclude that the reaction between  $\text{DMM}\cdot\text{IY}$  and  $[\text{Co}(\text{TPP})]$  results in formation of the unprecedented  $N$ -enolate-carbene radical species  $\text{I}^{\text{E-T}}$  (Scheme 3).

Additional proof for the structure of  $\text{I}^{\text{E-T}}$  comes from NMR and single-crystal X-ray diffraction (SC-XRD) characterization of the diamagnetic  $N$ -enolate-alkyl species  $\text{I}^{\text{A-E}}$ , which is readily obtained by HAT to the carbene radical moiety of  $\text{I}^{\text{E-T}}$

(Scheme 3). For more details about the formation and characterization of diamagnetic complex  $\mathbf{I}^{\text{A-E}}$ , see section “HAT-induced catalyst deactivation” (vide infra).

Having characterized the novel *N*-enolate-carbene radical intermediate  $\mathbf{I}^{\text{E-T}}$ , we proceeded to investigate its potential role in the catalytic reaction with styrene. As such, we exposed  $[\text{Co}(\text{TPP})]$  to 2 eq. of  $\text{DMM}\cdot\text{IY}$  to form  $\mathbf{I}^{\text{E-T}}$  in a quantitative manner, after which an excess of styrene (5 eq.) was added. To our surprise this “single-turnover” experiment produced 2 equivalents of cyclopropane **1**, thus indicating that both the carbene radical moiety *and* the enolate moiety of  $\mathbf{I}^{\text{E-T}}$  can each be transferred as a carbene group to styrene (Scheme 3). Clearly, and in stark contrast with the results of Mansuy obtained with closed-shell  $\text{Co}^{\text{III}}$ -porphyrins, formation of the *N*-enolate moiety is reversible for  $[\text{Co}^{\text{II}}(\text{TPP})]$ , and is not a catalyst deactivation pathway. Armed with this knowledge,  $\mathbf{I}^{\text{E-T}}$  was exposed to 1 eq. of styrene in a single-turnover reaction and studied by X-band EPR spectroscopy (Figure 4A). Interestingly, this produced a spectrum indicative of a cobalt-bound but organic-centered radical that is distinctly different from  $\mathbf{I}^{\text{E-T}}$ . Simulation ( $g_{11} = 2.018$ ;  $g_{22} = 1.988$ ;  $g_{33} = 2.047$ .  $A^{Co_{11}} = 15$ ,  $A^{Co_{22}} = 30$ ;  $A^{Co_{33}} = 135$  MHz) in comparison to the computed EPR parameters suggest the formation of *mono*-terminal carbene species  $\mathbf{I}^{\text{T}}$  (Figure S12 and Table S9, Supp. Inf.).

These findings suggest that the initial carbene transferred from  $\mathbf{I}^{\text{E-T}}$  to styrene is the carbene radical moiety, after which the *N*-enolate moiety of the newly formed  $\text{Co}^{\text{II}}$ -*N*-enolate adduct  $\mathbf{I}^{\text{E}}$  rearranges to  $\mathbf{I}^{\text{T}}$ . In the presence of additional styrene, the latter subsequently reacts to produce a second equivalent of cyclopropane (Scheme 3). Expanding on this hypothesis, we surmised that the order of addition, i.e.  $\{(1) \text{DMM}\cdot\text{IY}, (2) \text{styrene}, (3) [\text{Co}(\text{TPP})]\}$  or rather  $\{(1) \text{DMM}\cdot\text{IY}, (2) [\text{Co}(\text{TPP})], (3) \text{styrene}\}$ , might play a role in whether the *N*-enolate-carbene radical species  $\mathbf{I}^{\text{E-T}}$  or rather the *mono*-carbene radical  $\mathbf{I}^{\text{T}}$  is the dominant intermediate in the catalytic cycle. Indeed, when running the catalytic reaction by adding the reagents in the order  $\{(1) \text{DMM}\cdot\text{IY}, (2) [\text{Co}(\text{TPP})], (3) \text{styrene}\}$ , followed by freeze quenching the reaction mixture after 20 seconds, produced a mixture containing mainly  $[\text{Co}(\text{TPP})]$  and the *mono*-carbene radical species  $\mathbf{I}^{\text{T}}$  (Figure 4B), while upon reversing the order of addition to  $\{(1) \text{DMM}\cdot\text{IY}, (2) [\text{Co}(\text{TPP})], (3) \text{styrene}\}$  we detected a new, previously unencountered species. The relatively large *g*-anisotropy of the latter species points to a cobalt-centered radical, and based on a comparison with DFT calculated EPR parameters we ascribe this spectrum to the *N*-enolate adduct  $\mathbf{I}^{\text{E}}$  ( $g_{11} = 2.051$ ;  $g_{22} = 2.168$ ;  $g_{33} = 2.027$ .  $A^{Co_{11}} = -109$ ,  $A^{Co_{22}} = -124$ ;  $A^{Co_{33}} = 390$  MHz) (Figure 4C; Scheme 3). These data suggest that in reactions where the catalyst reacts first with the ylide, carbene transfer proceeds mostly from the *N*-enolate-carbene radical intermediate  $\mathbf{I}^{\text{E-T}}$ , while in reactions wherein styrene is present from the beginning

the *mono*-carbene radical  $\mathbf{I}^{\text{T}}$  is the dominant carbene transfer intermediate.

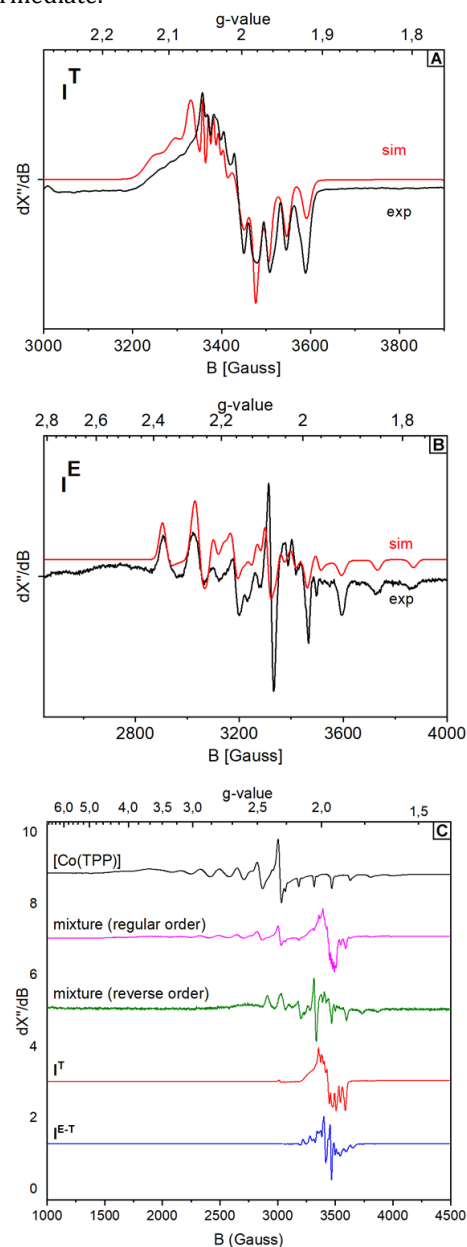


**Figure 4.** (A) X-band EPR spectrum of  $\mathbf{I}^{\text{T}}$  obtained in toluene- $d_8$  glass at 40 K after reacting  $\mathbf{I}^{\text{E-T}}$  with 1 eq. of styrene (microwave freq. 9.6443 GHz, mod. amp. 5 G, and power 6.325 mW). (B) EPR spectrum of  $\mathbf{I}^{\text{E}}$  measured after freeze quenching the catalytic reaction mixture obtained in the ‘reverse order’ of addition:  $\{(1) \text{DMM}\cdot\text{IY}, (2) [\text{Co}(\text{TPP})], (3) \text{styrene}\}$  (microwave freq. = 9.643446 GHz, mod. amp. = 4 G, power 0.6325 mW). (C) EPR spectra measured after freeze quenching the catalytic reaction mixtures obtained with two orders of addition, ‘regular order’  $\{(1) \text{DMM}\cdot\text{IY}, (2) \text{styrene}, (3) [\text{Co}(\text{TPP})]\}$  and ‘reverse order’  $\{(1) \text{DMM}\cdot\text{IY}, (2) [\text{Co}(\text{TPP})], (3) \text{styrene}\}$ , compared to the spectra of  $[\text{Co}(\text{TPP})]$ ,  $\mathbf{I}^{\text{T}}$  and  $\mathbf{I}^{\text{E-T}}$ .

We decided to gather more information about the nucleophilicity of the above detected intermediates via Hammett analysis of the carbene-transfer reactions (p. S53-S55, Supp.

Inf.). The Hammett plots were obtained under the optimized reactions conditions (Table 1, entry 13). To ensure complete conversion of all styrenes, the reaction time was extended to 15 min. To account for radical contributions to the Hammett parameters, the  $\sigma_{JJ}^\bullet$  radical spin-delocalization substituents<sup>37a</sup> were included as well as the classical  $\sigma^{+/-}$  Hammett constants.<sup>37b</sup> Plotting  $\log(k_x/k_H)$  vs  $\{\rho^\bullet\sigma_{JJ}^\bullet + \rho^-\sigma^- + C\}$  via multiple linear regression gave the best fit overall (Figure 5). Changing the order of addition of reagents does not have a noticeable influence on the obtained Hammett parameters (Figures S53–54 and Tables S13–14, Supp. Inf.), suggesting that both carbene radicals ( $\mathbf{I}^{\text{E-T}}$  and  $\mathbf{I}^\bullet$ ) have similar electronic properties. The necessary addition of  $\sigma_{JJ}^\bullet$ -values for an accurate fit supports the previously established radical character. Interestingly, the large  $|\rho^-/\rho^\bullet|$  values suggest a significant buildup of *negative charge* in the transition state. For  $|\rho^-/\rho^\bullet|$  values close to or greater than unity, electronic effects dominate and this implies that the carbene radicals are distinctly nucleophilic. This is in line with previously reported reactivity of  $\text{Co}^{\text{III}}$ -carbene radicals towards electron-deficient alkenes.<sup>9j,20a</sup>

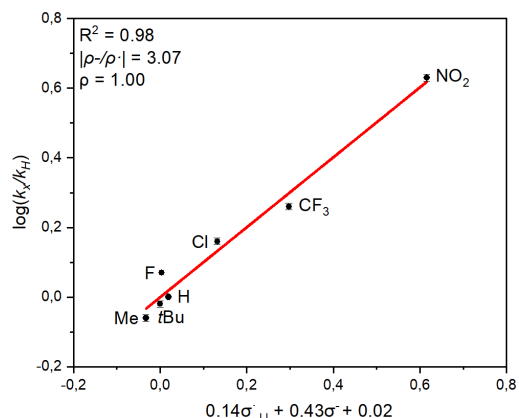


**Figure 5.** Hammett plot for the [Co(TPP)]-catalyzed cyclopropanation of styrene using DMM•IY.

**HAT-induced catalyst deactivation:** Cobalt(III)-carbene radicals are known to deactivate rapidly through hydrogen-atom-transfer (HAT) from either the starting diazo reagent or the solvent.<sup>9b,21</sup> Thus far, mechanistic studies of these deactivation processes have focused entirely on *mono*-substituted carbenes generated from diazo reagents. We therefore decided to investigate if similar deactivation processes also play a role for disubstituted carbene radicals generated from iodonium ylides. Detailed spectroscopic (EPR, NMR, UV/Vis, ATR-FT-IR) and mass spectrometric studies (p. S47-S48, Supp. Inf.) revealed that HAT from the solvent (toluene) or other hydrogen sources (e.g. trace impurities) indeed leads to deactivation of both *mono*-carbene radical intermediate  $\mathbf{I}^\bullet$  and *N*-enolate carbene radical intermediate  $\mathbf{I}^{\text{E-T}}$  to produce alkyl species  $\mathbf{I}^{\text{A}}$  and  $\mathbf{I}^{\text{E-A}}$ , respectively (Scheme 3). HAT-deactivation is observed to be faster for  $\mathbf{I}^\bullet$  than for  $\mathbf{I}^{\text{E-T}}$ , in good agreement with supporting DFT studies (p. S84, Supp. Inf.). The *N*-enolate moiety clearly has a protective function, making the barrier for HAT-deactivation higher. The diamagnetic alkyl species  $\mathbf{I}^{\text{E-A}}$

could be isolated and was characterized in detail by  $^1\text{H}$ -,  $^{13}\text{C}$ -,  $^1\text{H}^1\text{H}$ -COSY,  $^1\text{H}^{13}\text{C}$ -HSQC and HMBC NMR spectroscopy (p. S8-S9 & S62-65 Supp. Inf.) and single-crystal X-ray diffraction studies (p. S10, Supp. Inf.). NMR studies, bond-length analysis and use of the harmonic oscillator model for aromaticity<sup>38</sup> reveal that while TPP *N*-enolate functionalization leads to desymmetrization of the macrocycle, the overall aromaticity is largely retained (HOMA value: 0.91; p.S12, Supp. Inf.). The modified pyrrole ring binds to cobalt, but has a substantially elongated Co–N bond. Based on the bond distances, the *N*-enolate moiety has a delocalized negative charge.

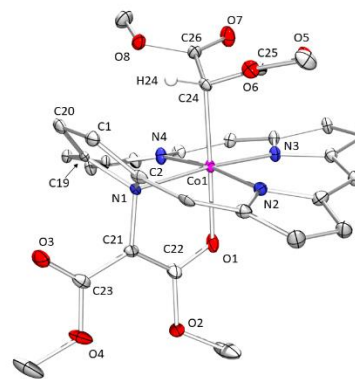


**Figure 6.** Solid-state crystal structure of  $\mathbf{I}^{\text{E-A}}$  at 100 K (ORTEP, thermal ellipsoids at 50% probability level). TPP phenyl groups, solvent molecules, disordered  $\text{O}_2$ -CH<sub>3</sub> positions and all protons except H24 omitted for clarity. Selected bond lengths (Å): Co1–N1 2.1195(17), Co1–N2 1.9700(18), Co1–N3 1.9464(17), Co1–N4 1.9752(16), Co1–O1 1.952(2), Co1–C24 2.045(2), N1–C21 1.489(3), C2–N1 1.464(3), C2–C1 1.381(3), C1–C20 1.396(3), C20–C19 1.387(3), C19–N1 1.457(3), C21–C22 1.400(4), C21–C23 1.441(3), C22–O1 1.260(3), C22–O2 1.416(4), C23–O3 1.217(3), C23–O4 1.356(3), C24–C25 1.486(3), C24–C26 1.486(3), C25–O5 1.206(3), C26–O7 1.213(3), C26–O8 1.351(3).

**Computational DFT studies:** To gain further insight into the mechanism of the metalloradical-catalyzed cyclopropanation reaction we turned to density functional theory calculations. Calculations were performed at the BP86/def2-TZVP level of theory, using Grimme's D3 dispersion corrections ('zero' damping), at the doublet spin surface. This method has been properly benchmarked against experimental data for cobalt(II)-porphyrin systems.<sup>12-16, 39-40</sup> The results are shown in Scheme 4. A detailed account is provided in the supporting information (p. S72, Supp. Inf.). Herein we summarize the main results, in direct comparison with the experimental data:

(a) The overall reaction mechanism for [Co(TPP)]-catalyzed styrene cyclopropanation is quite intricate, and consists of two interconnected catalytic cycles; a "*mono*-carbene cycle" in which *mono*-carbene radical complex  $\mathbf{I}^\bullet$  is the key intermediate, and a "*bis*-carbene cycle" in which *N*-enolate-carbene radical  $\mathbf{I}^{\text{E-T}}$  is the key carbene transfer intermediate. (b) Conversion of [Co(TPP)] to  $\mathbf{I}^\bullet$  and subsequent reaction of  $\mathbf{I}^\bullet$  with an additional equivalent of DMM•IY to produce  $\mathbf{I}^{\text{E-T}}$  both proceed via low barrier transition states, which are readily accessible at RT. The *mono*-terminal carbene radical

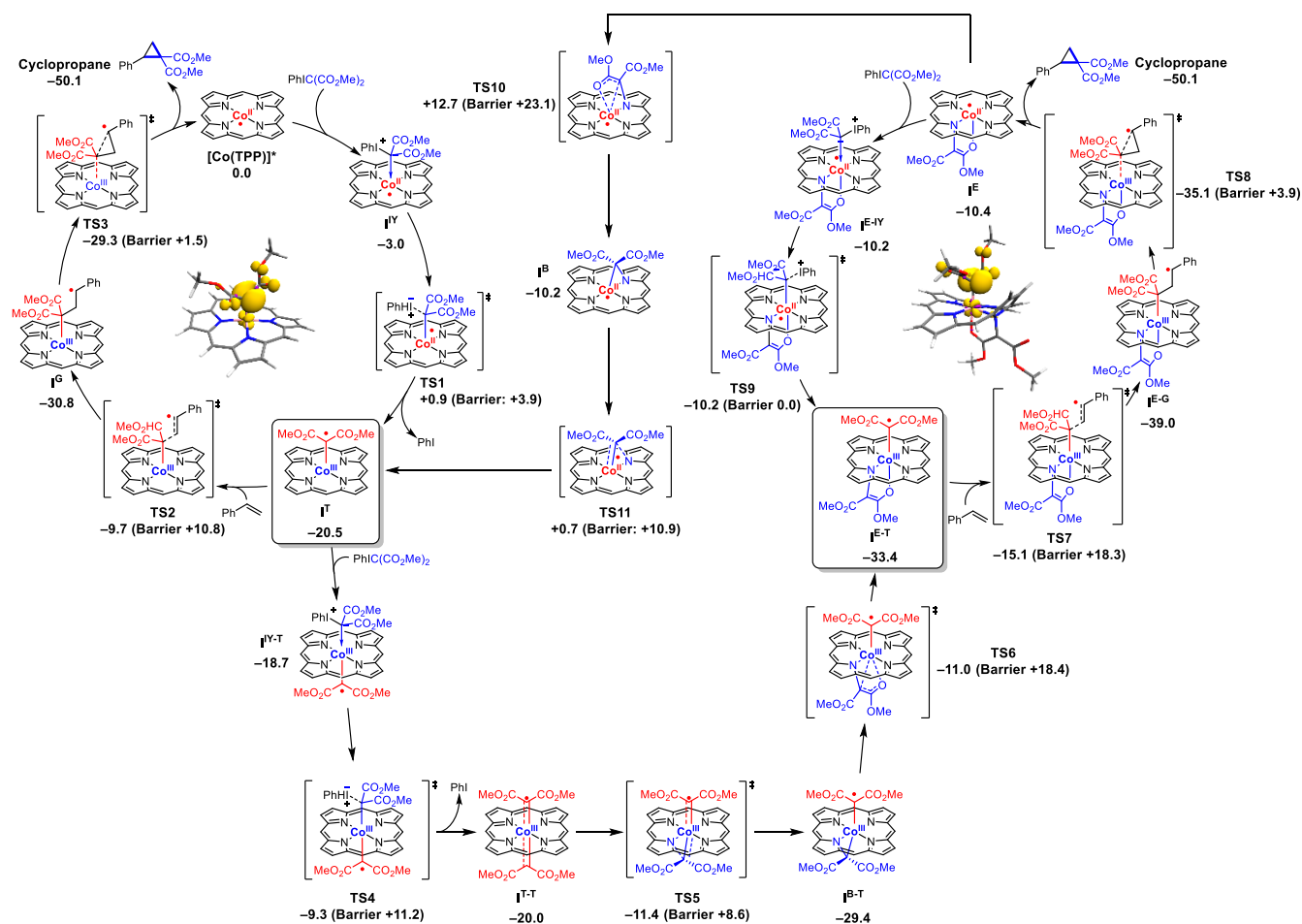
species  $\mathbf{I}^T$  is lower in energy than the *mono*-bridged carbene species  $\mathbf{I}^B$  and the *mono*-enolate adduct  $\mathbf{I}^E$ .<sup>41</sup> In contrast, the *N*-enolate-carbene radical species  $\mathbf{I}^{E-T}$  is more stable than the *bis*-terminal carbene species  $\mathbf{I}^{T-T}$ . These data are in agreement with the experimental observations (p. S47, Supp. Inf.).

(c) The “*bis*-carbene cycle” is reconnected to the “*mono*-carbene cycle” via intramolecular rearrangement of  $\mathbf{I}^B$  to  $\mathbf{I}^T$ , followed by formation of  $\mathbf{I}^T$ . The highest barrier of this process (TS10:  $\Delta\Delta G^\ddagger = +23.1$  kcal·mol<sup>-1</sup>) is readily accessible at RT, but this process should be relatively slow. It is in fact the highest barrier of the entire catalytic double-cycle, which explains why  $\mathbf{I}^E$  is detectable with EPR spectroscopy in trapping experiments (Figure 4C). These data are in excellent agreement with the experimental data, showing that *N*-enolate formation is reversible and that 2 eq. of cyclopropane are generated upon reaction of stoichiometrically generated  $\mathbf{I}^{E-T}$  with 5 eq. styrene.

(d) The barrier for styrene addition to  $\mathbf{I}^T$  is substantially lower than the barrier for styrene addition to  $\mathbf{I}^{E-T}$  (+10.8 vs. +18.3 kcal·mol<sup>-1</sup>). Conversely, activation of the iodonium ylide is barrierless for the “*bis*-carbene cycle”, whereas this

has a small barrier in the “*mono*-carbene cycle”. Since styrene addition is the rate-determining step in both cycles, the “*mono*-carbene cycle” should be faster than the “*bis*-carbene cycle”. Since the ylide is much less soluble than styrene, this implies that the *mono*-carbene cycle is likely to be the dominant catalytic pathway under reaction conditions where all components are present before adding the catalyst. Experimentally, this is indeed what is observed, because  $\mathbf{I}^T$  is detected as the resting state (Figure 4B) when adding the catalyst to the premixed reagents.<sup>42</sup>

(e) Formation of  $\mathbf{I}^{E-T}$  from *mono*-carbene radical  $\mathbf{I}^T$  is competitive with styrene addition to  $\mathbf{I}^T$  at equimolar concentrations (+11.2 vs. +10.8 kcal·mol<sup>-1</sup>), and hence both cycles are relevant. Experimentally we observed that in absence of styrene the reaction proceeds cleanly to  $\mathbf{I}^{E-T}$  at RT, and the “*bis*-carbene cycle” is clearly connected to the “*mono*-carbene cycle” (Figure 4A). While accessible at RT, the computed barrier for formation of  $\mathbf{I}^T$  from  $\mathbf{I}^E$  is relatively high (Scheme 4). Hence, in the presence of enough iodonium ylide DMM•IY the reaction should be largely trapped in the “*bis*-carbene cycle”. Experimental detection of  $\mathbf{I}^E$  with EPR



**Scheme 4.** Full catalytic cycle for the [Co(TPP)]-catalyzed reaction of DMM•IY and styrene. Free energies ( $\Delta G^\circ_{298K}$  in kcal·mol<sup>-1</sup>) are reported relative to the *mono*- and *bis*-benzene adducts of [Co(TPP)] for 5- and 6-coordinate species, respectively. All calculations were performed at the BP86/def2-TZVP/disp3 (m4-grid) level of theory at the doublet spin surface ( $S = \frac{1}{2}$ ). Inset figures show spin density plots of  $\mathbf{I}^T$  (left) and  $\mathbf{I}^{E-T}$  (right). Phenyl rings of the TPP ligand omitted for clarity.

spectroscopy for a reaction carried out by adding the reagents in the order *{(1) DMM•IY, (2) [Co(TPP)], (3) styrene}* (see Figure 4) confirms this.<sup>42</sup>

(f) Experimentally, the reaction between [Co(TPP)] and DMM•IY proceeds cleanly towards  $I^{E-T}$  without detectable amounts of  $I^T$  (Figure 1B). Computationally, the barrier for formation of  $I^T$  is lower than the barrier for formation of  $I^{E-T}$  (although both are very low), thus suggesting that  $I^T$  should in principle be detectable in titrations. This apparent discrepancy can be explained by the heterogeneous nature of the reaction mixture (Figure S20, Supp. Inf.). Moreover, hypervalent iodine reagents are known to form polymeric/oligomeric linear  $I^+-X^-$  chains,<sup>43</sup> and as such rapid and selective formation of “bis-carbene” species  $I^{E-T}$  with clear isobestic points in the titration experiments may well be the result of a high local concentration of ylide leading to rapid conversion of  $I^T$  to  $I^{E-T}$ .

**Comparison with the diazo analogue DMM•N<sub>2</sub>:** From a comparison of the computational pathways it becomes clear why the conventional diazo precursor DMM•N<sub>2</sub> is much less reactive toward [Co(TPP)] than the iodonium ylide DMM•IY (p. S89, Supp. Inf.). Formation of the initial ylidic coordination adduct is exergonic for DMM•IY with coordination of the central carbon as the most stable isomer. In contrast, the diazo compound coordinates most favorably via the carbonyl oxygen, although all adducts are uphill in energy (Scheme S14, Supp. Inf.). Moreover, expulsion of iodobenzene proceeds with a very low barrier (+3.9 kcal·mol<sup>-1</sup>) whereas the barrier for N<sub>2</sub>-loss from the diazo compound is much larger (+20.4 kcal·mol<sup>-1</sup>). However, activation of DMM•N<sub>2</sub> should still be possible based on these computational results. The calculated activation barrier for this process may therefore be somewhat underestimated, as experimentally no reaction is observable at room temperature within 1 h. A prolonged run at 60°C for 60 h produced less than 10% product, suggesting that carbene formation and subsequent transfer to styrene is possible with DMM•N<sub>2</sub> (Figures S51–52, Supp. Inf.). Nonetheless, no signals belonging to [Co(TPP)] were detectable and instead a diamagnetic fingerprint indicative of [Co<sup>III</sup>(TPP)]-alkyl species were found. Combined with the low yields obtained under the forcing conditions this suggests that catalyst deactivation plays a significant role with DMM•N<sub>2</sub> as a substrate.

**NEVPT2-CASSCF electronic structure calculations:** To check for possible multireference/multiconfigurational contributions to the electronic structures of the key carbene transfer intermediates  $I^T$  and  $I^{E-T}$ ,<sup>44</sup> and to provide an accurate description of their frontier molecular orbitals, we also performed NEVPT2-corrected CASSCF calculations (see Supp. Inf.). These calculations confirm that these species have a doublet ( $S = \frac{1}{2}$ ) ground state without significant multireference character, well-separated from higher spin states, and that their electronic structures are properly described by DFT. A detailed analysis of their NEVPT2-CASSCF electronic structure and a graphical representation of the energy-scaled frontier orbitals is provided in Tables S27–S28 and Figures S73–S74.

**Conclusions:** In this work we demonstrated that the acceptor-acceptor iodonium ylide DMM•IY is a highly suitable

precursor to generate, detect and characterize disubstituted carbene radicals at [Co(TPP)], which are productive in carbene transfer catalysis, and enable efficient and fast catalytic cyclopropanation of styrenes. Reaction of [Co(TPP)] with 2 eq. of DMM•IY produces the unprecedented *N*-enolate-carbene radical intermediate  $I^{E-T}$ , containing a Co<sup>III</sup>-carbene radical moiety and an enolate-modified porphyrin ring generated by carbene attack at one of the pyrrole rings of the TPP ligand. This species was unequivocally characterized with several spectroscopic methods and on the basis of its follow-up reactivity, providing a detailed picture of its (electronic) structure. In contrast to what might be expected, formation of the *N*-enolate is a reversible process, and not a route to catalyst deactivation. The carbene radical and the *N*-enolate moieties are both carbene-delivering functionalities capable of carbene transfer to other substrates.

Based on a combination of several spectroscopic, experimental and computational methods we conclude that the mechanism of the cyclopropanation reaction proceeds via two interconnected catalytic cycles. The key carbene transfer intermediate in one cycle is *mono*-carbene  $I^T$ , and in the other cycle it is the novel and unusual *N*-enolate-carbene radical  $I^{E-T}$ . Catalyst deactivation involves HAT from the solvent or trace impurities to the carbene radical moieties of these intermediates. Control experiments show that the DMM•N<sub>2</sub> reagent is catalytically inert under the optimized reaction conditions. Additional computational insight reveals DMM•N<sub>2</sub> to exhibit a significantly higher activation barrier than DMM•IY as well as unfavorable coordination minima for carbene formation. The interplay of opposing stabilities between terminal and *N*-bridging carbene (radical) moieties dictated by the Co<sup>II/III</sup>-redox cycle plays an important role, and explains the unique active participation of the otherwise catalytically inactive *N*-enolate species. Consequently, for these acceptor-acceptor carbenes, solvent-based hydrogen atom transfer is the dominant mode of deactivation. The *N*-enolate moiety clearly has a protective function, making the barrier for HAT-deactivation higher. Facile and energetically favorable carbene formation coupled with comparably high deactivation barriers leads to the observed highly selective formation of donor-acceptor cyclopropanes in quantitative yield. We envision that further application of these unique Co<sup>III</sup>-carbene radicals has the potential to unlock new scaffolds via the superior facile activation of acceptor-acceptor iodonium ylides over diazo compounds.

## ASSOCIATED CONTENT

### Supporting Information

The Supporting Information is available free of charge at [<link>](#). Experimental details; synthetic procedures; catalytic studies; XRD, EPR, NMR, UV-Vis, in-situ ATR-FT-IR and CSI+-MS spectroscopic data, DFT and NEVPT2-CASSCF calculations (PDF).

## AUTHOR INFORMATION

### Corresponding Author

**Bas de Bruin** – Homogeneous, Supramolecular and Bio-inspired Catalysis Group, University of Amsterdam, 1098 XH Amsterdam, The Netherlands

Email: [b.debruin@uva.nl](mailto:b.debruin@uva.nl)

### ORCID

Bas de Bruin: 0000-0002-3482-7669

Simon Mathew: 0000-0003-2480-3222

### Authors

**Roel F.J. Epping** – Homogeneous, Supramolecular and Bio-inspired Catalysis Group, University of Amsterdam, 1098 XH Amsterdam, The Netherlands

**Mees M. Hoeksma** – Homogeneous, Supramolecular and Bio-inspired Catalysis Group, University of Amsterdam, 1098 XH Amsterdam, The Netherlands

**Eduard O. Bobylev** – Homogeneous, Supramolecular and Bio-inspired Catalysis Group, University of Amsterdam, 1098 XH Amsterdam, The Netherlands

**Simon Mathew** – Homogeneous, Supramolecular and Bio-inspired Catalysis Group, University of Amsterdam, 1098 XH Amsterdam, The Netherlands

### Notes

The authors declare no competing financial interest.

## ACKNOWLEDGEMENTS

Financial support from The Netherlands Organization for Scientific Research (NWO TOP-Grant 716.015.001 to B.d.B.) is gratefully acknowledged. We thank David Vesseur and Nicolaas P. van Leest for fruitful discussions and Felix J. de Zwart for assistance with the EPR measurements.

## REFERENCES

- (1) (a) Sambiagio, C.; Schönbauer, D.; Blicek, R.; Dao-Huy, T.; Pototschnig, G.; Schaaf, P.; Wiesinger, T.; Zia, M. F.; Wencel-Delord, J.; Besset, T.; et al. A Comprehensive Overview of Directing Groups Applied in Metal-Catalysed C–H Functionalisation Chemistry. *Chem. Soc. Rev.* **2018**, *47* (17), 6603–6743. (b) Gensch, T.; Hopkinson, M. N.; Glorius, F.; Wencel-Delord, J. Mild Metal-Catalyzed C–H Activation: Examples and Concepts. *Chem. Soc. Rev.* **2016**, *45* (10), 2900–2936. (c) Gandeepan, P.; Müller, T.; Zell, D.; Cera, G.; Warratz, S.; Ackermann, L. 3d Transition Metals for C–H Activation. *Chem. Rev.* **2019**, *119* (4), 2192–2452. (d) Crabtree, R. H.; Lei, A. Introduction: CH Activation. *Chem. Rev.* **2017**, *117* (13), 8481–8482.
- (2) (a) Nakamura, I.; Yamamoto, Y. Transition-Metal-Catalyzed Reactions in Heterocyclic Synthesis. *Chem. Rev.* **2004**, *104* (5), 2127–2198. (b) Huang, C. Y.; Doyle, A. G. The Chemistry of Transition Metals with Three-Membered Ring Heterocycles. *Chem. Rev.* **2014**, *114* (16), 8153–8198.
- (3) (a) Doyle, M. P. Catalytic Methods for Metal Carbene Transformations. *Chem. Rev.* **1986**, *86* (5), 919–939. (b) Doyle, M. P.; Duffy, R.; Ratnikov, M.; Zhou, L. Catalytic Carbene Insertion into C–H Bonds. *Chem. Rev.* **2010**, *110* (2), 704–724. (c) Moss, R. A.; Doyle, M. P. Contemporary Carbene Chemistry. *Contemp. Carbene Chem.* **2013**, 1–566. (d) Zhu, D.; Chen, L.; Fan, H.; Yao, Q.; Zhu, S. Recent Progress on Donor and Donor–Donor Carbenes. *Chem. Soc. Rev.* **2020**, *49* (3), 908–950. (e) Xia, Y.; Qiu, D.; Wang, J. Transition-Metal-Catalyzed Cross-Couplings through Carbene Migratory Insertion. *Chem. Rev.* **2017**, *117* (23), 13810–13889.
- (4) (a) Davies, H. M. L.; Morton, D. Guiding Principles for Site Selective and Stereoselective Intermolecular C–H Functionalization by Donor/Acceptor Rhodium Carbenes. *Chem. Soc. Rev.* **2011**, *40* (4), 1857–1869. (b) Davies, H. M. L.; Liao, K. Dirhodium Tetracarboxylates as Catalysts for Selective Intermolecular C–H Functionalization. *Nat. Rev. Chem.* **2019**, *3* (6), 347–360.
- (5) (a) Maas, G. Ruthenium-Catalysed Carbenoid Cyclopropanation Reactions with Diazo Compounds. *Chem. Soc. Rev.* **2004**, *33* (3), 183–190. (b) Alcaide, B.; Almendros, P.; Luna, A. Grubbs' Ruthenium-Carbenes beyond the Metathesis Reaction: Less Conventional Non-Metathetic Utility. *Chem. Rev.* **2009**, *109* (8), 3817–3858.
- (6) (a) Kirmse, W. Copper Carbene Complexes: Advanced Catalysts, New Insights. *Angew. Chem. Int. Ed.* **2003**, *42* (10), 1088–1093. (b) Zhao, X.; Zhang, Y.; Wang, J. Recent Developments in Copper-Catalyzed Reactions of Diazo Compounds. *Chem. Commun.* **2012**, *48* (82), 10162–10173.

(7) (a) Damiano, C.; Sonzini, P.; Gallo, E. Iron Catalysts with N-Ligands for Carbene Transfer of Diazo Reagents. *Chem. Soc. Rev.* **2020**, *49* (14), 4867–4905. (b) Liu, Y.; You, T.; Wang, H. X.; Tang, Z.; Zhou, C. Y.; Che, C. M. Iron- And Cobalt-Catalyzed C(sp<sup>3</sup>)-H Bond Functionalization Reactions and Their Application in Organic Synthesis. *Chem. Soc. Rev.* **2020**, *49* (15), 5310–5358. (c) Intrieri, D.; Carminati, D. M.; Gallo, E. The Ligand Influence in Stereoselective Carbene Transfer Reactions Promoted by Chiral Metal Porphyrin Catalysts. *Dalt. Trans.* **2016**, *45* (40), 15746–15761. (d) Batista, V. F.; G A Pinto, D. C.; Silva, A. M. S. Iron: A Worthy Contender in Metal Carbene Chemistry. *ACS Catal.* **2020**, *10* (17), 10096–10116.

(8) (a) Dzik, W. I.; Zhang, X. P.; de Bruin, B. Redox Noninnocence of Carbene Ligands: Carbene Radicals in (Catalytic) C–C Bond Formation. *Inorg. Chem.* **2011**, *50* (20), 9896–9903. (b) Te Grotenhuis, C.; de Bruin, B. Radical-Type Reactions Controlled by Cobalt: From Carbene Radical Reactivity to the Catalytic Intermediacy of Reactive o-Quinodimethanes. *Synlett* **2018**, *29* (17), 2238–2250. (c) van Leest, N. P.; Epping, R. F. J.; van Vliet, K. M.; Lankelma, M.; van den Heuvel, E. J.; Heijtbrink, N.; Broersen, R.; de Bruin, B. Single-Electron Elementary Steps in Homogeneous Organometallic Catalysis, 1st ed.; Elsevier Inc., 2018; Vol. 70.

(9) **Cyclopropanes:** (a) Huang, L.; Chen, Y.; Gao, G. Y.; Zhang, X. P. Diastereoselective and Enantioselective Cyclopropanation of Alkenes Catalyzed by Cobalt Porphyrins. *J. Org. Chem.* **2003**, *68* (21), 8179–8184. (b) Penoni, A.; Wanke, R.; Tollari, S.; Gallo, E.; Musella, D.; Ragaini, F.; Demartin, F.; Cenini, S. Cyclopropanation of Olefins with Diazoalkanes, Catalyzed by Co<sup>II</sup>(Porphyrin) Complexes – A Synthetic and Mechanistic Investigation and the Molecular Structure of Co<sup>III</sup>(TPP)(CH<sub>2</sub>CO<sub>2</sub>Et) (TPP = Dianion of Meso-Tetraphenylporphyrin). *Eur. J. Inorg. Chem.* **2003**, No. 7, 1452–1460. (c) Zhu, S.; Ruppel, J. V.; Lu, H.; Wojtas, L.; Zhang, X. P. Cobalt-Catalyzed Asymmetric Cyclopropanation with Diazosulfones: Rigidification and Polarization of Ligand Chiral Environment via Hydrogen Bonding and Cyclization. *J. Am. Chem. Soc.* **2008**, *130* (15), 5042–5043. (d) Fantauzzi, S.; Gallo, E.; Rose, E.; Raoul, N.; Caselli, A.; Issa, S.; Ragaini, F.; Cenini, S. Asymmetric Cyclopropanation of Olefins Catalyzed by Chiral Cobalt(II)-Binaphthyl Porphyrins. *Organometallics* **2008**, *27* (23), 6143–6151. (e) Xu, X.; Lu, H.; Ruppel, J. V.; Cui, X.; Mesa, S. L. De; Wojtas, L.; Zhang, X. P. Highly Asymmetric Intramolecular Cyclopropanation of Acceptor-Substituted Diazoacetates by Co(II)-Based Metalloradical Catalysis: Iterative Approach for Development of New-Generation Catalysts. *J. Am. Chem. Soc.* **2011**, *133* (39), 15292–15295. (f) Intrieri, D.; Caselli, A.; Gallo, E. Cyclopropanation Reactions Mediated by Group 9 Metal Porphyrin Complexes. *Eur. J. Inorg. Chem.* **2011**, No. 33, 5071–5081. (g) Ruppel, J. V.; Cui, X.; Xu, X.; Zhang, X. P. Stereoselective Intramolecular Cyclopropanation of  $\alpha$ -Diazoacetates via Co(II)-Based Metalloradical Catalysis. *Org. Chem. Front.* **2014**, *1* (5), 515–520. (h) Otte, M.; Kuipers, P. F.; Troeppner, O.; Ivanović-Burmazović, I.; Reek, J. N. H.; de Bruin, B. Encapsulated Cobalt-Porphyrin as a Catalyst for Size-Selective Radical-Type Cyclopropanation Reactions. *Chem. Eur. J.* **2014**, *20* (17), 4880–4884. (i) Goswami, M.; de Bruin, B.; Dzik, W. I. Difluorocarbene Transfer from a Cobalt Complex to an Electron-Deficient Alkene. *Chem. Commun.* **2017**, *53* (31), 4382–4385. (j) Chirila, A.; Gopal Das, B.; Paul, N. D.; de Bruin, B. Diastereoselective Radical-Type Cyclopropanation of Electron-Deficient Alkenes Mediated by the Highly Active Cobalt(II) Tetramethyltetraaza[14]Annulene Catalyst. *ChemCatChem* **2017**, *9* (8), 1413–1421. (k) Wang, Y.; Wen, X.; Cui, X.; Wojtas, L.; Zhang, X. P. Asymmetric Radical Cyclopropanation of Alkenes with in Situ-Generated Donor-Substituted Diazo Reagents via Co(II)-Based Metalloradical Catalysis. *J. Am. Chem. Soc.* **2017**, *139* (3), 1049–1052. (l) Roy, S.; Das, S. K.; Chattopadhyay, B. Cobalt(II)-Based Metalloradical Activation of 2-(Diazomethyl)Pyridines for Radical Transannulation and Cyclopropanation. *Angew. Chemie – Int. Ed.* **2018**, *57* (8), 2238–2243. (m) Lee, W.-C. C.; Wang, D.-S. Zhang, C.; Xie, J.; Li, B.; Zhang, X. P.

Asymmetric radical cyclopropanation of dehydroaminocarboxylates: Stereoselective synthesis of cyclopropyl- $\alpha$ -amino acids. *Chem.* **2021**, *7*, 1–14.

(10)  **$\beta$ -Lactams:** (a) Paul, N. D.; Chirila, A.; Lu, H.; Zhang, X. P.; de Bruin, B. Carbene Radicals in Cobalt(II)-Porphyrin-Catalyzed Carbene Carbonylation Reactions; A Catalytic Approach to Ketenes. *Chem. – A Eur. J.* **2013**, *19* (39), 12953–12958. (b) Chirila, A.; van Vliet, K. M.; Paul, N. D.; de Bruin, B. [Co(MeTAA)] Metalloradical Catalytic Route to Ketenes via Carbonylation of Carbene Radicals. *Eur. J. Inorg. Chem.* **2018**, (20), 2251–2258.

(11) **Indenes:** Das, B. G.; Chirila, A.; Tromp, M.; Reek, J. N. H.; de Bruin, B. Co<sup>III</sup>-Carbene Radical Approach to Substituted 1H-Indenes. *J. Am. Chem. Soc.* **2016**, *138* (28), 8968–8975.

(12) **Chromenes:** (a) Paul, N. D.; Mandal, S.; Otte, M.; Cui, X.; Zhang, X. P.; de Bruin, B. Metalloradical Approach to 2H-Chromenes. *J. Am. Chem. Soc.* **2014**, *136* (3), 1090–1096. (b) Majumdar, N.; Paul, N. D.; Mandal, S.; de Bruin, B.; Wulff, W. D. Catalytic Synthesis of 2H-Chromenes. *ACS Catal.* **2015**, *5* (4), 2329–2366.

(13) **Piperidines:** Lankelma, M.; Olivares, A. M.; de Bruin, B. [Co(TPP)]-Catalyzed Formation of Substituted Piperidines. *Chem. Eur. J.* **2019**, *25* (22), 5658–5663.

(14) **Cyclooctenes:** (a) te Grotenhuis, C.; van den Heuvel, N.; van der Vlugt, J. I.; de Bruin, B. Catalytic Dibenzocyclooctene Synthesis via Cobalt(III)-Carbene Radical and Ortho-Quinodimethane Intermediates. *Angew. Chem, Int. Ed.* **2018**, *57* (1), 140–145. (b) Zhou, M.; Lankelma, M.; van der Vlugt, J. I.; de Bruin, B. Catalytic Synthesis of 8-Membered Ring Compounds via Cobalt(III)-Carbene Radicals. *Angew. Chem. Int. Ed.* **2020**, *59* (27), 11073–11079.

(15) **Dienes:** Te Grotenhuis, C.; Das, B. G.; Kuipers, P. F.; Hageman, W.; Trouwborst, M.; de Bruin, B. Catalytic 1,2-Dihydronaphthalene and E-Aryl-Diene Synthesis via Co<sup>III</sup>-Carbene Radical and o-Quinodimethane Intermediates. *Chem. Sci.* **2017**, *8* (12), 8221–8230.

(16) **Indolines:** (a) Karns, A. S.; Goswami, M.; de Bruin, B. Catalytic Synthesis of Indolines by Hydrogen Atom Transfer to Cobalt(III)-Carbene Radicals. *Chem. Eur. J.* **2018**, *24* (20), 5253–5258. (b) Wen, X.; Wang, Y.; Zhang, X. P. Enantioselective Radical Process for Synthesis of Chiral Indolines by Metalloradical Alkylation of Diverse C(sp<sup>3</sup>)-H Bonds. *Chem. Sci.* **2018**, *9* (22), 5082–5086.

(17) **Furans:** Cui, X.; Xu, X.; Wojtas, L.; Kim, M. M.; Zhang, X. P. Regioselective Synthesis of Multisubstituted Furans via Metalloradical Cyclization of Alkynes with  $\alpha$ -Diazocarbonyls: Construction of Functionalized  $\alpha$ -Oligofurans. *J. Am. Chem. Soc.* **2012**, *134* (49), 19981–19984.

(18) **Pyrrolidines:** Wang, Y.; Wen, X.; Cui, X.; Zhang, X. P. Enantioselective Radical Cyclization for Construction of 5-Membered Ring Structures by Metalloradical C–H Alkylation. *J. Am. Chem. Soc.* **2018**, *140* (14), 4792–4796.

(19) **Alkenes:** Lee, M. Y.; Chen, Y.; Zhang, X. P. General and Selective Olefination of Aldehydes and Ketones Catalyzed by a Cobalt(II) Porphyrin Complex. *Organometallics* **2003**, *22* (24), 4905–4909.

(20) (a) Dzik, W. I.; Xu, X.; Zhang, X. P.; Reek, J. N. H.; de Bruin, B. Carbene Radicals in Co<sup>II</sup>(Por)-Catalyzed Olefin Cyclopropanation. *J. Am. Chem. Soc.* **2010**, *132* (31), 10891–10902. (b) Lu, H.; Dzik, W. I.; Xu, X.; Wojtas, L.; de Bruin, B.; Zhang, X. P. Experimental Evidence for Cobalt(III)-Carbene Radicals: Key Intermediates in Cobalt(II)-Based Metalloradical Cyclopropanation. *J. Am. Chem. Soc.* **2011**, *133* (22), 8518–8521. (c) Ikeno, T.; Iwakura, I.; Yamada, T. Cobalt-Carbene Complex with Single-Bond Character: Intermediate for the Cobalt Complex-Catalyzed Cyclopropanation. *J. Am. Chem. Soc.* **2002**, *124* (51), 15152–15153.

(21) Chirila, A.; Brands, M. B.; de Bruin, B. Mechanistic Investigations into the Cyclopropanation of Electron-Deficient Alkenes with Ethyl Diazoacetate Using [Co(MeTAA)]. *J. Catal.* **2018**, *361*, 347–360.

(22) (a) Chen, Y.; Fields, K. B.; Zhang, X. P. Bromoporphyrins as Versatile Synthons for Modular Construction of Chiral Porphyrins: Cobalt-Catalyzed Highly Enantioselective and Diastereoselective Cyclopropanation. *J. Am. Chem. Soc.* **2004**, *126* (45), 14718–14719. (b) Ruppel, J. V.; Jones, J. E.; Huff, C. A.; Kambale, R. M.; Chen, Y.; Zhang, X. P. A Highly Effective Cobalt Catalyst for Olefin Aziridination with Azides: Hydrogen Bonding Guided Catalyst Design. *Org. Lett.* **2008**, *10* (10), 1995–1998. (c) Hu, Y.; Lang, K.; Tao, J.; Marshall, M. K.; Cheng, Q.; Cui, X.; Wojtas, L.; Zhang, X. P. Next-Generation D<sub>2</sub>-Symmetric Chiral Porphyrins for Cobalt(II)-Based Metal-radical Catalysis: Catalyst Engineering by Distal Bridging. *Angew. Chem. Int. Ed.* **2019**, *58* (9), 2670–2674. (d) Zhu, S.; Perman, J. A.; Zhang, X. P. Acceptor/Acceptor-Substituted Diazo Reagents for Carbene Transfers: Cobalt-Catalyzed Asymmetric Z-Cyclopropanation of Alkenes with  $\alpha$ -Nitrodiazoacetates. *Angew. Chemie – Int. Ed.* **2008**, *47* (44), 8460–8463.

(23) (a) Yoshimura, A.; Zhdankin, V. V. Advances in Synthetic Applications of Hypervalent Iodine Compounds. *Chem. Rev.* **2016**, *116* (5), 3328–3435. (b) Yusubov, M. S.; Yoshimura, A.; Zhdankin, V. V. Iodonium Ylides in Organic Synthesis. *Arkivoc* **2016**, *2016* (1), 342–374.

(24) (a) Goudreau, S. R.; Marcoux, D.; Charette, A. B. General Method for the Synthesis of Phenyliodonium Ylides from Malonate Esters: Easy Access to 1,1-Cyclopropane Diesters. *J. Org. Chem.* **2009**, *74* (1), 470–473. (b) Goudreau, S.R.; Marcoux, D.; Charette, A. B. Synthesis of Dimethyl 2-Phenylcyclopropane-1,1-Dicarboxylate Using an Iodonium Ylide Derived From Dimethyl Malonate. *Org. Synth.* **2010**, *87*, 115. (c) Zhu, C.; Yoshimura, A.; Ji, L.; Wei, Y.; Nemykin, V. N.; Zhdankin, V. V. Design, Preparation, X-Ray Crystal Structure, and Reactivity of  $o$ -Alkoxyphenyliodonium Bis(Methoxycarbonyl)Methanide, a Highly Soluble Carbene Precursor. *Org. Lett.* **2012**, *14* (12), 3170–3173. (d) Ochiai, M.; Tada, N.; Okada, T.; Sota, A.; Miyamoto, K. Thermal and Catalytic Transylidations between Halonium Ylides and Synthesis and Reaction of Stable Aliphatic Chloronium Ylides. *J. Am. Chem. Soc.* **2008**, *130* (7), 2118–2119. (e) Geary, G. C.; Hope, E. G.; Singh, K.; Stuart, A. M. Preparation of Iodonium Ylides: Probing the Fluorination of 1,3-Dicarbonyl Compounds with a Fluoroiodane. *RSC Adv.* **2015**, *5* (21), 16501–16506. (f) Zhu, C.; Yoshimura, A.; Solntsev, P.; Ji, L.; Wei, Y.; Nemykin, V. N.; Zhdankin, V. V. New Highly Soluble Dimerone-Derived Iodonium Ylides: Preparation, X-Ray Structure, and Reaction with Carbodiimide Leading to Oxazole Derivatives. *Chem. Commun.* **2012**, *48* (81), 10108–10110. (g) Cardinale, J.; Ermert, J. Simplified Synthesis of Aryliodonium Ylides by a One-Pot Procedure. *Tetrahedron Lett.* **2013**, *54* (16), 2067–2069.

(25) (a) Zhao, R.; Shi, L. Reactions between Diazo Compounds and Hypervalent Iodine(III) Reagents. *Angew. Chem. Int. Ed.* **2020**, *59* (30), 12282–12292. (b) Okuyama, T.; Takino, T.; Sueda, T.; Ochiai, M. Solvolysis of Cyclohexenyliodonium Salt, a New Precursor for the Vinyl Cation: Remarkable Nucleofugality of the Phenyliodonio Group and Evidence for Internal Return from an Intimate Ion—Molecule Pair. *J. Am. Chem. Soc.* **1995**, *117* (12), 3360–3367.

(26) (a) Lee, Y. R.; Cho, B. S. Rhodium(II)-Catalyzed Reaction of Iodonium Ylides with Heterocyclic and Aromatic Compounds. Efficient Synthesis of Fused Acetals and C–H Insertion Products. *Bull. Korean Chem. Soc.* **2002**, *23* (5), 779–782. (b) Müller, P.; Boléa, C. The Enantioselectivity and the Stereochemical Course of Copper-Catalyzed Intramolecular CH Insertions of Phenyliodonium Ylides. *Helv. Chim. Acta* **2002**, *85* (2), 483–494. (c) Vaitla, J.; Hopmann, K. H.; Bayer, A. Rhodium-Catalyzed Synthesis of Sulfur Ylides via in Situ Generated Iodonium Ylides. *Org. Lett.* **2017**, *19* (24), 6688–6691. (d) Adam, W.; Bosio, S. G.; Gogonas, E. P.; Hadjiarapoglou, L. P. A Stereoselective and Regioselective Synthesis of Trans,Trans-Configured 1,2,3-Trisubstituted Indanes: Cycloaddition of Alkenes with Iodonium Ylides of  $\beta$ -Disulfones. *Synthesis* **2002**, *14*, 2084–2090. (e) Müller, P. Asymmetric Transfer of Carbenes with Phenyliodonium Ylides. *Acc. Chem. Res.* **2004**, *37* (4), 243–251. (f) Lee, Y.

R.; Jung, Y. U. Efficient Synthesis of  $\beta$ -Substituted  $\alpha$ -Haloenones by Rhodium(II)-Catalyzed and Thermal Reactions of Iodonium Ylides. *J. Chem. Soc. Perkin Trans. 1* **2002**, No. 10, 1309–1313. (g) Adam, W.; Gogonas, E. P.; Hadjiarapoglou, L. P. A Remarkable Cycloaddition of Bis(Arylsulfonyl)Iodonium Ylide with Norbornene Derivatives for the Direct Synthesis of Functionalized Indanes. *Synlett* **2003**, No. 8, 1165–1169. (h) Karche, N. P.; Jachak, S. M.; Dhavale, D. D. Electronic Effects in Migratory Groups. [1,4]- versus [1,2]-Rearrangement in Rhodium Carbenoid Generated Bicyclic Oxonium Ylides. *J. Org. Chem.* **2001**, *66* (19), 6323–6332. (i), 470–473. (j) Lee, Y. R.; Yoon, S. H.; Seo, Y.; Kim, B. S. Rhodium(II)-Catalyzed Reaction of Iodonium Ylides with Conjugated Compounds: Efficient Synthesis of Dihydrofurans, Oxazoles, and Dihydrooxepines. *Synthesis* **2004**, *17*, 2787–2798. (k) Wurz, R. P.; Charette, A. B. Hypervalent Iodine(III) Reagents as Safe Alternatives to  $\alpha$ -Nitro- $\alpha$ -Diazocarbonyls. *Org. Lett.* **2003**, *5* (13), 2327–2329. (l) Muller, P.; Ghanem, A. Rh(II)-Catalyzed Enantioselective Cyclopropanation of Olefins with Dimethyl Malonate via in Situ Generated Phenyliodonium Ylide. *Org. Lett.* **2004**, *6* (23), 4347–4350. (m) Batsila, C.; Gogonas, E. P.; Kostakis, G.; Hadjiarapoglou, L. P. Alkenyl C–H Insertion of Iodonium Ylides into Pyrroles: Studies toward the Total Syntheses of Tolmetin and Amlolmetin Guacil. *Org. Lett.* **2003**, *5* (9), 1511–1514. (n) Lee, Y.; Yoon, S. Rhodium(II)-Catalyzed Reaction of Iodonium Ylides with Electron-Deficient and Conjugated Alkynes: Efficient Synthesis of Substituted Furans. *Synth. Commun.* **2006**, *36* (14), 1941–1951. (o) Bonge, H. T.; Hansen, T. Rhodium(II) Catalyzed Three-Component Coupling: A Novel Reaction of in Situ Generated Iodonium Ylides. *Tetrahedron Lett.* **2008**, *49* (1), 57–61. (p) Vaid, R.K.; Hopkins, T.E. Use of an Iodonium Ylide in the Synthesis of  $p$ -Nitrobenzyl-(6R,7S)-hydroxy-8-oxo-7-phenoxyacetamido-1-azabicyclo[4.2.0]octa-2-ene-2-carboxylate. *Tetrahedron Lett.* **1997**, *38* (40), 6981–6984. (q) Adam, W.; Gogonas, E. P.; Hadjiarapoglou, L. P. A Facile Diastereoselective Synthesis of Functionalized 1,2,3-Trisubstituted Benzocyclopentenes through the Cycloaddition of Bis(Phenylsulfonyl)Iodonium Ylides to Cyclic Alkenes. *J. Org. Chem.* **2003**, *68* (23), 9155–9158.

(27) (a) Moriarty, R. M.; May, E. J.; Prakash, O. Intramolecular Cyclization of Aryl Substituted Iodonium Ylides with Copper(I) Chloride. *Tet. Lett.* **1997**, *38* (25), 4333–4336. (b) Deng, C.; Wang, L. J.; Zhu, J.; Tang, Y. A Chiral Cagelike Copper(I) Catalyst for the Highly Enantioselective Synthesis of 1,1-Cyclopropane Diesters. *Angew. Chem. Int. Ed.* **2012**, *51* (46), 11620–11623. (c) Chidley, T.; Murphy, G. K. Cyclopropanation of Alkenes with Metallocarbenes Generated from Monocarbonyl Iodonium Ylides. *Org. Biomol. Chem.* **2018**, *16* (44), 8486–8490. (d) Liang, H.; He, X.; Zhang, Y.; Chen, B.; Ouyang, J. S.; Li, Y.; Pan, B.; Subba Reddy, C. V.; Chan, W. T. K.; Qiu, L. Copper-Catalyzed (4+1) and (3+2) Cyclizations of Iodonium Ylides with Alkynes. *Chem. Commun.* **2020**, *56* (77), 11429–11432. (e) Wang, H. X.; Li, W. P.; Zhang, M. M.; Xie, M. S.; Qu, G. R.; Guo, H. M. Synthesis of Chiral Pyrimidine-Substituted Diester D–A Cyclopropanes: Via Asymmetric Cyclopropanation of Phenyliodonium Ylides. *Chem. Commun.* **2020**, *56* (78), 11649–11652. (f) Ho, P. E.; Tao, J.; Murphy, G. K. Wittig Reagents as Metallocarbene Precursors: In Situ Generated Monocarbonyl Iodonium Ylides. *Eur. J. Org. Chem.* **2013**, *29*, 6540–6544. (g) Mo, S.; Li, X.; Xu, J. In Situ-Generated Iodonium Ylides as Safe Carbene Precursors for the Chemoselective Intramolecular Buchner Reaction. *J. Org. Chem.* **2014**, *79* (19), 9186–9195. (h) Müller, P.; Boléa, C. Enantioselective Intramolecular CH-Insertions upon Cu-Catalyzed Decomposition of Phenyliodonium Ylides. *Molecules* **2001**, *6* (3), 258–266. (i) Müller, P.; Boléa, C. Asymmetric Induction in Cu-Catalyzed Intramolecular Cyclopropanations of Phenyliodonium Ylides. *Synlett* **2000**, No. 6, 826–828. (j) Paizanos, K.; Charalampou, D.; Kourkoumelis, N.; Kalpogianaki, D.; Hadjiarapoglou, L.; Spanopoulou, A.; Lazarou, K.; Manos, M. J.; Tasiopoulos, A. J.; Kubicki, M.; et al. Synthesis and Structural Characterization of New Cu(I) Complexes with the Antithyroid Drug 6–

n-Propyl-Thioureas. Study of the Cu(I)-Catalyzed Intermolecular Cycloaddition of Iodonium Ylides toward Benzo[b]Furans with Pharmaceutical Implementations. *Inorg. Chem.* **2012**, *51* (22), 12248–12259.

(28) (a) Besenyei, G.; Neszmélyi, A.; Holly, S.; Simándi, L. I.; Párkányi, L. A Relationship between the Catalytic Carbonylation of (N-Arenesulfonyl)Imides and Iodonium Ylides. *Can. J. Chem.* **2001**, *79* (5–6), 649–654. (b) Li, W. G.; Cai, B.; Xiao, H. B.; Pi, S. F.; Sun, H. Z. Palladium-Catalyzed Dehydrogenation Coupling-Cyclization Reactions of Acetylenic Acids with Iodonium Ylides for the Synthesis of 2-(5H)-Furanones. *Synlett* **2016**, *27* (5), 794–798. (c) Pradhan, S.; Mishra, K.; Lee, Y. R. Support-Free Pd<sub>3</sub>Co NCs as an Efficient Heterogeneous Nanocatalyst for New Organic Transformations of C–C Coupling Reactions. *Chem. Eur. J.* **2019**, *25* (46), 10886–10894.

(29) Miyazawa, T.; Suzuki, T.; Kumagai, Y.; Takizawa, K.; Kikuchi, T.; Kato, S.; Onoda, A.; Hayashi, T.; Kamei, Y.; Kamiyama, F.; et al. Chiral Paddle-Wheel Diruthenium Complexes for Asymmetric Catalysis. *Nat. Catal.* **2020**, *3* (10), 851–858.

(30) (a) Guo, J.; Liu, Y.; Li, X.; Liu, X.; Lin, L.; Feng, X. Nickel(II)-Catalyzed Enantioselective Cyclopropanation of 3-Alkenyl-Oxindoles with Phenyliodonium Ylide via Free Carbene. *Chem. Sci.* **2016**, *7* (4), 2717–2721. (b) Guo, J.; Liu, X.; He, C.; Tan, F.; Dong, S.; Feng, X. Nickel(II)-Catalyzed Enantioselective  $\alpha$ -Alkylation of  $\beta$ -Ketoamides with Phenyliodonium Ylide via a Radical Process. *Chem. Commun.* **2018**, *54* (86), 12254–12257.

(31) Thus far, investigations into the application of iodonium ylides as metal carbene precursors in catalysis have focused almost entirely on Rh- and Cu-based systems with fruitful forays into Pd, Ru and Ni.

(32)(a) Mansuy, D.; Battioni, J. P.; Akhrem, I.; Dupré, D.; Fischer, J.; Weiss, R.; Morgenstern-Badarau, I. Reaction of a Carbon Analogue of Iodosylbenzene with Iron Porphyrins: Isolation and X-Ray Structure of an Iron(II) Complex with O–C–C Moieties Inserted between Two Trans Iron–Nitrogen Bonds. *J. Am. Chem. Soc.* **1984**, *106* (20), 6112–6114. (b) Battioni, J. P.; Artaud, I.; Dupre, D.; Leduc, P.; Akhrem, I.; Mansuy, D.; Fischer, J.; Weiss, R.; Morgenstern-Badarau, I. Reaction of a Carbon Equivalent of Iodosylbenzene with Iron–Porphyrins: A Ready Access to N-Alkylporphyrin Complexes Involving Five-Membered Fe–O–C–C–N Metallocycles. *J. Am. Chem. Soc.* **1986**, *108* (18), 5598–5607. (c) Battioni, J. P.; Artaud, I.; Dupre, D.; Leduc, P.; Mansuy, D. Preparation and Properties of Iron(II), Cobalt(III), and Zinc(II) N-Alkylporphyrin Complexes Involving Five-Membered Metal–O–C=C–N Metallocycles. *Inorg. Chem.* **1987**, *26* (11), 1788–1796. (d) Artaud, I.; Gregoire, N.; Battioni, J. P.; Dupre, D.; Mansuy, D. Heme Model Studies Related to Cytochrome P-450 Reactions: Preparation of Iron–Porphyrin Complexes with Carbenes Bearing a  $\beta$ -Oxygen Atom and Their Transformation into Iron–N-Alkylporphyrins and Iron–Metallocyclic Complexes. *J. Am. Chem. Soc.* **1988**, *110* (26), 8714–8716.

(33)(a) Cui, X.; Xu, X.; Jin, L. M.; Wojtas, L.; Zhang, X. P. Stereoselective Radical C–H Alkylation with Acceptor/Acceptor-Substituted Diazo Reagents via Co(II)-Based Metalloradical Catalysis. *Chem. Sci.* **2015**, *6* (2), 1219–1224. (b) Xu, X.; Wang, Y.; Cui, X.; Wojtas, L.; Zhang, X. P. Metalloradical Activation of  $\alpha$ -Formyldiazoacetates for the Catalytic Asymmetric Radical Cyclopropanation of Alkenes. *Chem. Sci.* **2017**, *8* (6), 4347–4351.

(34) (a) Goswami, M.; Lyaskovskyy, V.; Domingos, S. R.; Buma, W. J.; Woutersen, S.; Troeppner, O.; Ivanović-Burmazović, I.; Lu, H.; Cui, X.; Zhang, X. P.; et al. Characterization of Porphyrin–Co(III)–‘nitrene Radical’ Species Relevant in Catalytic Nitrene Transfer Reactions. *J. Am. Chem. Soc.* **2015**, *137* (16), 5468–5479. (b) Van Leest, N. P.; Tepaske, M. A.; Oudsen, J. P. H.; Venderbosch, B.; Rietdijk, N. R.; Siegler, M. A.; Tromp, M.; Van Der Vlugt, J. I.; De Bruin, B. Ligand Redox Noninnocence in [Co<sup>III</sup>(TAML)]<sup>9/-</sup> Complexes Affects Nitrene Formation. *J. Am. Chem. Soc.* **2020**, *142* (1), 552–563. (c) Van Leest, N. P.; Tepaske, M. A.; Venderbosch, B.; Oudsen, J. P. H.; Tromp, M.; Van Der Vlugt, J. I.; De Bruin, B. Electronically Asynchronous Transition States for C–N Bond Formation by Electrophilic

[Co<sup>III</sup>(TAML)]–Nitrene Radical Complexes Involving Substrate-to-Ligand Single-Electron Transfer and a Cobalt-Centered Spin Shuttle. *ACS Catal.* **2020**, *10* (14), 7449–7463.

(35) In this work, we employ the term “carbenoid” as a general container term for bridging, enolate or terminal variants of metal carbenes in those places in the text where the structural assignment is not yet clear. For a more general discussion of the term “carbenoid”, see: Caballero, A.; Pérez, P. J. Dimensioning the Term Carbenoid. *Chem. - A Eur. J.* **2017**, *23* (58), 14389–14393.

(36) (a) Ikeno, T.; Iwakura, I.; Yamada, T. Cobalt–Carbene Complex with Single-Bond Character: Intermediate for the Cobalt Complex-Catalyzed Cyclopropanation. *J. Am. Chem. Soc.* **2002**, *124* (51), 15152–15153. (b) Setsune, J.; Iida, T.; Kitao, T. The Reaction of Cobalt(III)–Porphyrins with  $\alpha$ -Diazo- $\beta$ -Dicarbonyl Compounds. *Chem. Lett.* **1989**, 885–888.

(37) (a) Jiang, X. K. Establishment and Successful Application of the  $\sigma_{\text{H}}$  Scale of Spin-Delocalization Substituent Constants. *Acc. Chem. Res.* **1997**, *30* (7), 283–289. (b) Hansch, C.; Leo, A.; Taft, R. W. A Survey of Hammett Substituent Constants and Resonance and Field Parameters. *Chem. Rev.* **1991**, *91* (2), 165–195.

(38) Kruszewski, J.; Krygowski, T. M. Definition of Aromaticity Basing on the Harmonic Oscillator Model. *Tetrahedron Lett.* **1972**, *13* (36), 3839–3842.

(39) (a) de Bruin, B.; Dzik, W. I.; Li, S.; Wayland, B. B. Hydrogen-Atom Transfer in Reactions of Organic Radicals with [Co<sup>II</sup>(por)]. (por=Porphyrinato) and in Subsequent Addition of [Co(H)(por)] to Olefins. *Chem. Eur. J.* **2009**, *15*, 4312–4320. (b) Li, S.; Peng, C.-H.; Fryd, M.; Wayland, B. B.; de Bruin, B.; Exchange of Organic Radicals with Organo-Cobalt Complexes Formed in the Living Radical Polymerization of Vinyl Acetate. *J. Am. Chem. Soc.* **2008**, *130*, 13373–13381.

(40) Kuijpers, P. F.; Tiekink, M. J.; Breukelaar, W. B.; Broere, D. L. J.; van Leest, N. P.; van der Vlugt, J. I.; Reek, J. N. H.; de Bruin, B. Nitrene-radical approach to Saturated Heterocycles; Cobalt Porphyrin Catalyzed Intramolecular Ring-Closing C–H Amination of Aliphatic Azides. *Chem. Eur. J.* **2017**, *23*, 7945–7952.

(41) This result contrasts with the results obtained for *mono*-substituted carbenes, for which *mono*-bridged species of type **I<sup>B</sup>** are slightly favored over *mono*-terminal carbene radical species of type **I<sup>T</sup>**. See ref 20–21.

(42) The low solubility of DMM•IY has a significant influence on the (relative) rates though. Unfortunately, this also prevents reliable kinetic studies to determine condition dependent kinetic reaction orders to gain more experimental information about the relative importance of the “*mono*-carbene” and “*bis*-carbene” cycles.

(43) (a) Carmalt, C. J.; Crossley, J. G.; Knight, J. G.; Lightfoot, P.; Martin, A.; Muldowney, M. P.; Norman, N. C.; Orpen, A. G. An Examination of the Structures of Iodosylbenzene (PhIO) and the Related Imido Compound, PhINSO<sub>2</sub>-4-Me-C<sub>6</sub>H<sub>4</sub>, by X-Ray Powder Diffraction and EXAFS (Extended X-Ray Absorption Fine Structure) Spectroscopy. *J. Chem. Soc. Chem. Commun.* **1994**, No. 20, 2367–2368. (b) Macikenas, D.; Skrzypczak-Jankun, E.; Protasiewicz, J. D. A New Class of Iodonium Ylides Engineered as Soluble Primary Oxo and Nitrene Sources. *J. Am. Chem. Soc.* **1999**, *121*, 7164–7165. (c) Macikenas, D.; Skrzypczak-Jankun, E.; Protasiewicz, J. D. Redirecting Secondary Bonds to Control Molecular and Crystal Properties of an Iodosyl- and an Iodylbenzene. *Angew. Chemie - Int. Ed.* **2000**, *39* (11), 2007–2010. (d) Ivanov, A. S.; Popov, I. A.; Boldyrev, A. I.; Zhdankin, V. V. The I=X (X=O,N,C) Double Bond in Hypervalent Iodine Compounds: Is It Real? *Angew. Chemie - Int. Ed.* **2014**, *53* (36), 9617–9621.

(44) van Leest, N. P.; de Bruin, B. Revisiting the Electronic Structure of Cobalt–Porphyrin Nitrene and Carbene Radicals with NEVPT2-CASSCF Calculations: Doublet versus Quartet Ground States. *Inorg. Chem.* **2021**, in press. <https://doi.org/10.1021/acs.inorgchem.1c00910>.